#1 Review for WCD-2020-1 (RC1 from 11 Feb 2020)

This study describes an exceptional period of thunderstorm activity in western Europe during summer 2018 and explores the associated synoptic-scale conditions; in particular, the role of blocking and associated upstream cut-off lows. The event is also placed in a climatological context using long-term records from surface stations, upper-air soundings, and reanalysis.

This is an interesting, thorough and well-written piece of work, which I have no hesitation in recommending for publication, subject to a few minor revisions as detailed below. I would like to thank the authors for their efforts, which made for an easy and enjoyable review.

AC: We thank the reviewer for the time taken to review our manuscript and for the useful comments. We are pleased that the reviewer finds the manuscript an interesting, thorough and well-written piece of work.

Specific Comments:

1. My most significant comment relates to your conclusion regarding the slow movement of convective systems during the event. You provide clear evidence (in Fig. 9) that storm motion was, on average, much lower than is typically observed in this region and at this time of year and suggest that this was key to the extreme rainfall totals. However, storm motion is not the only relevant factor for heavy precipitation. As discussed by Doswell et al. (1996), accumulated rainfall depends on two things: average rain rate and total rainfall duration. Slow cell motion contributes to long rainfall durations, but one must also consider system size (in the direction or storm motion) and the existence of back-building convection, both of which may lead to echo training. Rainfall rates must also be considered. Given that you have hourly gauge data and radar observations, it should be possible to assess all of these things. While this might not be practical for the whole study period, you should consider doing so for the most extreme events noted in Table 1. One option would be to add an extra column to the table, providing a brief description of the storm(s) that caused the rainfall totals (including their estimated motion). At the very least, it would be good to demonstrate that the general characteristic of slow storm motion applies to some of the individual extreme events.
   AC: We responded this point of criticism by reviewing all German events in Table 1 again with RADOLAN data (merger between radar and station data), so that we were able to investigate the rain rate and duration in more detail (see Supplement Sect. 4 and Supplementary Figure 5). We added these values to Table 1, which impressively shows the particular high rain rate (e.g., 50 min over 60 mm/h for Dietenhofen). Furthermore, we included a discussion in Sect. 5 on that (also citing Doswell et al., 1996). Additionally, we added further information based on the TRACE3D algorithm in Table 1, which shows that many of the cells has a propagation speed below 7 m/s (only one of the sample has a propagation speed of more than 10 m/s). Note that due to data availability, these detailed analyses were only available for Germany.

2. You state in your abstract that low vertical wind shear “prevented thunderstorms from developing into severe organized systems”. However, reports of hail up to 5 cm in diameter (L234; L239) suggest that this is not entirely true. Clearly, wind shear in certain areas and on certain days was sufficient for the development of organised convection (probably supercells). As such I think this statement needs revising.
   AC: The correct formulation would have been that " the low-pressure gradient led predominantly to weak flow conditions in the mid-troposphere and thus to low vertical wind shear that prevented thunderstorms from developing into severe organized systems.” We changed that.
   Furthermore, we added a comment on the 5 cm hail stone (during the discussion of the ESWD reports): “…the wind shear values over the study area were predominantly very low. Individual cases with hail stones of 5 cm were feasible, because in the border area of our study area above the Pyrenees twice areas with high shear (up to 20 m/s) was transported, which led to the large hail in southwest France (26 May/9 June) or southern Germany (11 June). However, these were exceptional cases.“
   Note, even if there are many days with hail reports (Fig. 2), this does not necessarily mean that high shear

was necessary, since hail – but usually smaller hail – is also observed with low shear situations (see Kunz et al., 2020). Note 86 % of the hail events during the long investigation period are <= 3 cm.

2. Please provide some citations for reports of storm impacts (in the opening paragraph of the introduction and section 3.1). These could simply be links to online news or social media reports.
   AC: We included some references for the storm impacts based on WetterOnline and DWD online media reports (however, only in German):
   Tornado wütet bei Viersen: Dutzende Häuser stark beschädigt (17.05.2018)
   https://www.wetteronline.de/extremwetter/tornado-wuetet-bei-viersen-dutzende-haeuser-stark-beschaedigt-2018-05-17-tv
   Unwetterserie Ende Mai: Ganze Ortschaften verwüstet
   https://www.wetteronline.de/extremwetter/unwetterserie-ende-mai-ganze-ortschaften-verwuestet-2018-05-31-us
   Unwetterserie im Juni: Überflutungen und Hagelmassen
   https://www.wetteronline.de/extremwetter/unwetterserie-im-juni-ueberflutungen-und-hagelmassen-2018-06-14-js
   Schadensrückblick des Deutschen Wetterdienstes: Gefährliche Wetterereignisse und Wetterschäden in Deutschland 2018:
   https://www.dwd.de/DE/presse/pressemitteilungen/DE/2018/20181213_schadensrueckblick2018_news.html

3. The second paragraph of the introduction doesn't really fit and has only limited direct relevance to your study. As such I would suggest removing it (although parts of it could potentially be incorporated elsewhere in the introduction).
   AC: We fundamentally revised the introduction. On this occasion, there were some textual restructuring. The second paragraph was also rewritten and shortened. The aspect of thunderstorm development (we moved the ingredient-based theory from Sect. 6 into the introduction as suggested by the another reviewer) and the scale interactions (between local and large-scale) was still considered; but the link to teleconnection was removed. The latter is not relevant for this paper, and thus rather confusing at this point.

4. I know that 1981–2010 is a standard 30-year climatology period, but for this study you should consider using the full ERA-Interim record (1979–2017) in order to provide a more complete historical context for the 2018 event. I believe the sounding data will go back this far as well.

   AC: We wanted to use a consistent period of 30 years, which is homogenous in the different analyses in the paper calculating the climatological mean, as is common in several studies. When calculating the return periods (Fig. 13/15), where this aspect is important, we have already taken into account longer time series (more or less what was available).
   We tested this aspect regarding Fig. 14 & Fig. 16 (for 1981-2017). However, no significant differences were found, meaning that we kept to the previous period with a fixed annual period of 30 years.

5. On Line 140 you claim that surface-based lifted index (SLI) offers "the best representation of convective environmental conditions in central Europe". I would expect CAPE to provide a more robust measure of surface-based instability, given that it considers the full column rather than just a single level (see discussion in Doswell and Schultz 2006). Certainly it has been shown to usefully discriminate between severe and non-severe convective environments in various parts of the world, including Europe (Pucik et al. 2015; Taszarek et al. 2017). It is also available as a diagnostic from ERA-Interim, so could easily be analysed spatially as well as from the point soundings. I appreciate that repeating all of your instability analysis using CAPE would be time consuming and is likely to show comparable results, so I will not request this. However, you should provide some further justification for why you chose to use SLI over CAPE.

AC: For Europe, there are many studies showing that SLI can be used as well as CAPE (e.g., Huntrieser et al., 1997; Westermayer et al., 2017; Rädler et al., 2018; Sanchez et al., 2009). Some studies also showed that the skill to predict thunderstorms and/or their sub-peril can better as using CAPE (e.g., Kunz, 2007; Mohr and Kunz, 2013; Haklander and van Delden, 2003; Manzato, 2003;). In addition, CAPE has the disadvantage that its distribution function is skewed and that the CAPE values can be zero (or small) despite (high) instability in the atmosphere. Our experience (in our last studies) has shown that SLI is more robust in our different analyses, so we prefer to use it.
We added a comment on this. Additionally, we observed that the key messages in this paper do not change significantly when analyses are performed with CAPE.

6. You use a very high reflectivity threshold (55 dBZ) for identifying and tracking convective storms. Such a value is more characteristic of hail than intense rainfall. As such I wonder if the majority of storms went undetected, leading to an unrepresentative velocity estimate. One simple way to check this would be to see if the storms that produce some of the extreme rain accumulations listed in Table 1 were detected. At the very least this should be noted as a limitation of your radar-based analysis.
   AC: That's right, a threshold of 55 dBZ prevents weaker cells from entering the sample. However, as we are focusing here on heavy rainfall, this threshold is appropriate: We explained this in the text. "Note that we have only used tracking to estimate the propagation speed and direction of the cells (Sect. 3 and Sect. 5.1). Even if weaker cells are not detected using the 55 dBZ thresholds, it can be assumed that they cannot move at higher speeds."
   In addition, we checked if the German events in Table 1 can be linked with a track derived with TRACE3D and included the information of track length, propagation speed, and total track area in the Table. However, two tracks could not be identified by TRACE3D due to the overlapping of several cells, which were relatively quasi-stationary.

7. It would be good to include a figure showing the different weather regimes discussed in section 2.3 (or, at least, the ZO, EuBL, and AR regimes that dominated during the study period). Perhaps this can be found elsewhere. If so, please refer to the specific figure(s) in the relevant paper(s).
   AC: The illustration of the Atlantic-European weather regimes can be found in Grams et al., 2017 – however in the Supplementary information (Supplementary Figure 1); but only for the winter season, but which are very similar to the summer season.
   We now provided the typical patterns (for May/June) as supplementary material.

8. In discussing the persistence analysis in section 2.5, and the associated results in section 5.2, I found the reference to "cluster length" confusing, in part because K-Means clustering is used in the analysis of weather regimes. I would change this to just "event duration" or "event persistence".
   AC: We followed the suggestion and changed the formulation "cluster length" in "event persistence".

9. Could you provide a few more details on the origin of the "basic" and "strict" criteria for SLI and mid-tropospheric wind speed, so that the reader doesn't have to go to PIP16 for this information? Also, I'm not a fan of the notation TH BC and TH SC for these and would argue that they can be eliminated (you can just refer to the basic/strict criterion).
   AC: TH BC and TH SC are introduced in PIP16 – this is the reason why we used this notation here.
   We added a comment to the definition "Both thresholds were originally determined by choosing the maximum of the daily minima in the case study to capture the prevailing (exceptional) atmospheric conditions." and deleted the abbreviations/notation TH BC and TH SC in the text.

10. I recommend using V500 (rather than v 500hPa) to indicate the 500hPa wind speed.
    AC: We implemented this suggestion.

11. I suggest using "total" or "accumulation" when referring to precipitation amounts rather than "sum" (e.g. in Table 1 and on L260–261).

    AC: We implemented this suggestion and also unify the wording on this.

12. I'm confused as to why you focus the opening paragraph of section 3.3.1 and the first three panels of Fig. 4 on the two weeks before your main study period. In my view it would make more sense for Fig. 4 to show more regular snapshots from the study period, so that the reader can more easily see the temporal evolution described in the subsequent two paragraphs. In particular, it would be good to include one snapshot that shows the second cut-off low (C2) and one close to the end of the study period.
AC: We think it is important to highlight the synoptic situation also prior to the event in order to emphasise that the severe convection during the study period was embedded in a longer lasting unusual large-scale flow situation. The synoptic conditions prior to the event featured blocking, the formation of cut-off lows, and facilitated the advection of warm-moist air into central Europe, which was a key ingredient for the high-impact event. Therefore, we decided to keep the synoptic discussion of May/June along with the characterisation in terms of unusual geopotential height anomalies and IWV (Fig. 5) and the evolution of weather regimes (Fig. 6). As C2 did not strongly affect central Europe we compromised not to show it (now we state in line 296 "(C2, not shown)". Instead we provide a detailed synoptic discussion of the impact of C3 in section 4. We made this aspect clearer in the text.

13. In section 5.1, you note that several of the rainfall return period maxima in Fig. 13 "have an almost circular shape with the highest value located in the center" and suggest that this characteristic "reflects the very slow propagation of the thunderstorms". However, could it instead be an artefact of insufficient gauge density? If only one gauge recorded the event, this information would be spread laterally by the gridding procedure, giving the impression of a small circular shape. It might be worth overlaying the gauge locations on this plot to check how many gauges are associated with each maximum.
AC: REGNIE gridded data are based on approx. 2,000 stations (more or less all ground-based observation networks of DWD; see black points in the Fig.).
Comparing the stations with our estimated RPs shows that the majority of all events are captured by several stations and not by only one. We added a comment on that.

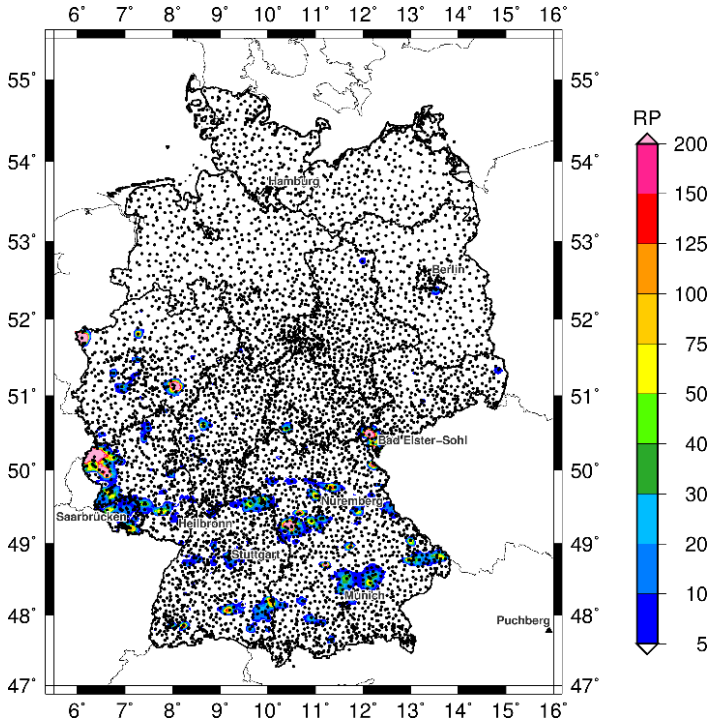

14. The description of Fig. 14 at the start of section 5.2 is rather confusing and should be revised. In particular, I found it hard to understand how the distributions for the climatological period were derived.
AC: We rewrote the description and hope that it is now more understandable and less confusing.

15. Several of the figures could be improved in a few ways. Specifically, I recommend the following changes:

    ○ Fig. 3: The top and bottom rows could arguably be combined. In this case, rather than colouring the symbols on the map by rainfall amount you could just make them blue for > 35 mm/h and red for > 60 mm/3h; then use these same colours for the bar plot (with red bars overlaid on blue bars).
    AC: We combined Figs. 3a and 3c in one histogram (good suggestion), so that the number of stations is easier to compare. However, we kept Fig. 3b and 3d separate, since this way a spatial representation of the maximum precipitation (especially for the 3 h panel) is maintained.

    ○ Fig. 7: I don't think it's necessary to state the two thresholds within the plots; this information can be provided in the caption (with reference to the dashed lines).
    AC: Personally, I'm a friend of putting a lot of information in figures (if they don't irritate too much), so

that – if the figure is used elsewhere – all information is included. However, we removed it and provide the info only in the figure caption.

○ Fig. 12: I would get rid of the hatching showing the objectively identified cut-offs and use a darker contour for the pressure vertical velocity.
AC: We revised the figure and hope that by leaving the blue colours (< 1PVU) it is now clearer.

○ Fig. 14: It would be helpful to use different colours for the box-and-whisker plots corresponding to the study period and the 1981–2010 climatology. Use the same colour convention for Fig. 9.
AC: We implemented this suggestion.

○ Fig. 15: In the legend, rather than putting "(2018: N days incl. M skip days)" for each station I would just put "(N/M)" and then explain what these numbers indicate in the caption. So, for example, for Essen you would put "(17/3)" instead of "(2018: 17 days incl. 3 skip days)".
AC: We implemented this suggestion.

○ Fig. 16: Rather than plotting the percentage difference from the climatological frequency (which is confusing because it is a percentage of a percentage), I recommend expressing this difference in terms of the standard deviation of the climatological frequency. This will highlight whether the 2018 frequencies were exceptional in the context of typical year-to-year variability.
AC: We concur, that a percentage of a percentage would be confusing. However, in Fig. 16 we show in shading the ((absolute frequency in May/June 2018)-climatological frequency May/June 1981-2010)). Thus, over Northern Spain absolute frequencies exceed 50 %, which would be relatively speaking a change of more than 1000 % compared to climatology. We clarified this in the figure caption.
"Climatological mean percentage of days with a cut-off low in May and June (black contours; every 2 %; for May and June 1981 – 2010) and anomaly percentage of days during the study period (shaded in % with reference to mean percentage of days} in May and June; ERA-Interim)".

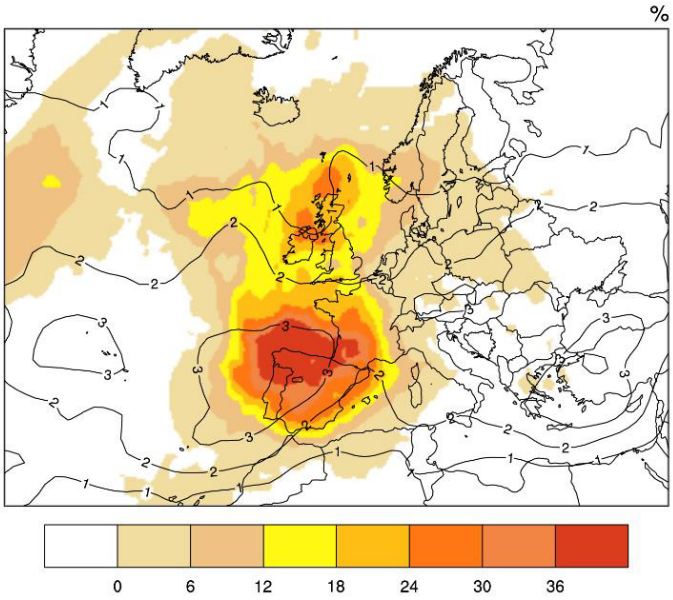

Furthermore, we checked the suggestion with the standard deviation of the cut-off low frequency and added a comment on that (however the added value of an extra figure for the std is too small to include; see Fig. here).

Technical Corrections

1. There are a few issues with tenses in the text. For example, the opening sentence of the introduction is written in the present perfect tense (use of "has been"), but should be in the past tense ("was"). The same goes for L261. The last sentence of the opening paragraph of section 3.3.3 is written in the simple present tense but should be in the past tense.
   AC: The manuscript was checked by an editor service; we included the improvements. Thanks for the careful reading.

2. L23: Parentheses are (are not) for references and clarification (saving space) (Robock 2010). Please modify this sentence accordingly.
   AC: We changed this as proposed.

3. L36: "...serve to precondition the thermodynamic environment."
   AC: We changed this.

16. L39–42: To which event are you referring here: 2018 or 2016? I suggest rewording this paragraph to make this clear. Similarly, you should state explicitly the event you are referring to on L71.
   AC: 2016. We clarified this in the text "During the episode in 2016…"

17. Line 60: Lifting will only lead to the release of CAPE (i.e. convective initiation) if it is sufficient for parcels of air to reach their level of free convection; however, it may still act to destabilise the column (increase CAPE) and erode lids (reduce CIN).
   AC: That's right. We added some words on this.
   "When such a positive PV filament moves over air masses that are conditionally or potentially unstably stratified, they trigger lifting and thereby release convective available potential energy (if the air parcel reach its level of free convection)} and facilitate/cause deep moist convection."

18. Line 90–91: Suggest revising the end of this sentence as follows: "...based on reports from storm chasers, eyewitnesses, voluntary observers, meteorological services, and news media."
   AC: We changed this as proposed.

19. L97–98: "... the Météo-France (1223/1935 stations with hourly/daily data)..."
   AC: We changed this as proposed.

20. Line 100: These are the national meteorological services of all the countries in your study so I don't think you need this last part of the sentence.
   AC: We deleted the last part.

21. Line 132: "wind speed and direction"
   AC: We changed this.

22. L146: What is the altitude of the lowest level?
   AC: 1 km above ground is the lowest level and 12 km the highest.

23. L199: Change "fewer" to "less".
   AC: We changed this.

24. L239–240: Suggest revising this sentence as follows: "Many of the record-breaking 1h and 3h rain totals occurred within this period (see Sect. 3.2)."
   AC: We implemented this suggestion.

25. L255–256: "...the latter on the day with the second most ESWD severe weather reports (cf. Sect. 3.1)." Rather than referring to the previous section here please specify the actual date.
   AC: We implemented this (31 May).

26. L257–258: You deal with the variations in large-scale forcing for convection later in the paper so I don't think it is necessary to include this here (unless you want to explicitly refer to the relevant sections).
   AC: We deleted the sentence.

27. L271: Change "were" to "where".
   AC: Thanks. We changed this.

28. L272–273: This sentence is confusing and should be revised.
   AC: We fundamentally revised and restructured the first part of Section 3 and deleted some passages. In doing so, the sentence was also deleted.

29. L357: Change "vast parts of" to "much of".
   AC: We changed this.

30. L362: Change "exemplarily shown for" to "exemplified by".
   AC: Good suggestion. We now used this formulation.

31. Line 380–381: Change “and was already mentioned at the end of Section 3.2” to just “(Section 3.2)”.
    We changed this.
32. L510: Advected where?
    AC: “into Europe”. We added this.
33. L526: Get rid of “(global/regional)”.
    AC: We deleted this.

#2 Review for WCD-2020-1 (RC1 from 23 Feb 2020)

Overview: The paper presents a case study of a long-lasting thunderstorm series over France/central Europe in May/June 2018 that occurred south of a blocking high. The synoptic situation persisted for several weeks. The thunderstorms were associated with cut-off lows/potential vorticity filaments that formed on the south-west of the blocking high. As a result, numerous severe convective events such as flash floods, hail and wind gusts were recorded. The authors use multiple different data sets and methods to show how the large-scale dynamics contribute to the thunderstorm series and that this event was exceptional.

Overall, I like the author's idea of studying this event from synoptic down to the convective scales. Moreover, it is an interesting case. However, I think the manuscript was difficult to follow and can still be improved considerably. In the current form, it was unfortunately no pleasure to read through the study. My main criticism is that large parts of the paper (chapter 2,3,4, but also in the introduction) read like a collection of single parts which are not really connected with one another.

A central theme seems to be missing.
AC: See Introduction Lines 76-80:
"The primary objective of this paper is to examine the conditions and processes that made this particular thunderstorm episode in 2018 unique. We focus on the process interaction across scales, i.e., from the large-scale dynamics such as atmospheric blocking to meso-scale PV cut-off lows and/or small meso-scale PV filaments to modifications of the convective environment to local-scale thunderstorm occurrences." For this purpose, it is also necessary to describe the "synoptic framework during the thunderstorm episode, to show the severity of the events and to place event in a historical context".

I think, the authors should restructure the paper or parts of it and follow a clear path, e.g. from large-scale to the small scale or the other way around. If this is not possible, they should at least clarify the purpose of each (!) chapter at the beginning (as it is done in chapter 5) to facilitate the reading.

AC: We edited and restructured several text passages, in particular we rewrote the introduction, restructured the sub-sections in Section 2 and rewrote the beginning of Section 3. Furthermore, we tried to link the text passages better with each other. We also split long sentences.

Moreover, in my opinion, the writing can be improved, too. Some sentences are too long, which makes the text hard to read. Just write necessary information and just reference to papers that are relevant for your topic. Make the sentences clear and concise. Please connect the single chapters and (sub)sections with one another!
AC: We split long sentences. Additionally, we connected the individual chapters better and included a more detailed description at the end of the introduction, so this should help the reader for the storyline.

I will explain my criticism in more detail in the following:

(i) In the introduction, the authors switch strongly between different topics: first they introduce the case and its impacts in a few sentences. Then they describe convective development due to scale interactions (mainly lifting processes). Afterwards they describe the case again with focus on blocking which is described more general thereafter. In the successive part, the authors explain cut-off lows in the potential vorticity framework. Afterwards they switch back to the topic of blocking. However, these single parts are often unconnected with one another which is confusing for the reader!
AC: We fundamentally revised the introduction. On this occasion, there were some textual restructuring, shortening, and additions and hope that all these (justified) criticised points are thus been eliminated.

(ii) In the data and methods chapter (chapter 2), data sources are often introduced without clarifying why the authors will need the data. At least some overview at the beginning of this section – how the study was designed and/or what data satisfies which purpose – would help the reader tremendously!

AC: We took this criticism into account and integrated the necessary information in the corresponding text passages (see also comments below).
Are there any new methods? Please clarify!
AC: Please, see comments below.

(iii) The same applies for chapters 3,4, and partly 5! Try to connect the single parts, try not to jump unnecessarily between topics. In the current version, it is really confusing for the reader.
AC: We edited several text passages to better structure aspects necessary for the individual chapters.

(iv) With respect to the methods my main concern is the usage of the 500hPa-wind instead of vertical wind shear. At least additionally analyzing shear had the advantage that your work can be compared more easily to the existing literature of convective events.
AC: We made a conscious decision to show V500 and not the shear (although we had already examined both). One reason for V500 was the connection with the propagation speed of the cells (see also the comment on propagation speed below), since our focus in the work was not to analyse the organizational structure of the cells using wind shear. Furthermore, the interesting point for us was the really extraordinary low wind speeds in the mid-troposphere.
In the panel of Figure 7 we now additionally included the bulk wind shear between 10 m and 500 hPa – showing that the values averaged over the study period are almost similar to V500. We added also some comments on that.

(v) Furthermore, I am missing evidence, that the thunderstorms have been single cells rather than multicells, MCS or slow-moving (HP) supercells.
AC: Separating the convective cells among their organization form might be an interesting issue, but is far beyond the content and aim of our paper. Furthermore, we do not have an algorithm that allows us to adequately identify this. We added animated images of radar reflectivity for two representative days in the video supplementary. These animations show how both single cells and multicells develop throughout the day. A brief discussion is included in Section 3. Furthermore, we weakened the statement about single cells and changed the wording into isolated cells (which clearly can be seen in the radar animations). Finally, we added some more information about the dimensions of the storms detected by the tracking algorithm to Table 1.

p. 16, lines 490-496: Especially since the precipitation amounts are so high, how do you know that the thunderstorms were mainly single cells? Moreover, did you mention at any point in your paper, how you differentiate between single cells and other convective thunderstorm types like multicells? Maybe you can put the radar movies for one of the extreme cases you talked about to the supplemental material?
AC: We followed the suggestion and included radar movies for two days (the most severe ones) in the supplementary. These animations show how both single cells and multicells develop throughout the day. A brief discussion is included in Section 3.1. Furthermore, we weakened the statement about single cells and changed the wording into isolated cells (which clearly can be seen in the radar animations). Finally, we added some more information about the dimensions of the storms detected by the tracking algorithm to Table 1.

Specific minor comments:

Abstract, p.1 line 2: "80mm" - what is the temporal range? a few hours?
AC: See Table 1. Theoretically several time scales are possible (1 h, but also in 3 h). We added an information in the abstract.

p.2, line 25-36: I am missing the general ingredients of convection here: instability, moisture, lift and shear. The ingredients-based concept is first mentioned in the Discussion chapter (chapter 6), I think it would be fitting in the introduction, too.
We moved the text passage on the ingredient-based theory of Sect. 6 to the introduction.
Moreover e.g.
Markowski and Richardson, 2010 (their chapter 10.4) &

Doswell III, C. A., Brooks, H. E., & Maddox, R. A. (1996): Flash flood forecasting: An ingredients-based methodology. Weather and Forecasting, 11(4), 560-581.
treat flash flood events. Especially in the Markowski and Richardson book, you can find a very similar synoptic pattern that led to flash flood events in the US (please refer to the publications mentioned therein).
AC: We decided to use the suggested references in the discussion section, because it fits best there.

p.2, line 34: "all these mechanisms" - which ones are meant here?
AC: In the course of a revision of the "introduction" this sentence was deleted.

p.2, lines 51-61: There are some publications concerning the PV framework and convection: e.g.
Russell A, Vaughan G, Norton EG. 2012. Large-scale potential vorticity anomalies and deep convection. Q. J. R. Meteorol. Soc. 138: 1627–1639. DOI:10.1002/qj.1875;
Morcrette CJ, Lean H, Browning KA, Nicol J, Roberts N, Clark PA, Russell A, Blyth AM. 2007. Combination of mesoscale and synoptic mechanisms for triggering of an isolated thunderstorm: a case study of CSIP IOP 1. Mon. Weather Rev. 135: 3728–3749.
Can you please put your work in context with the existing literature?
AC: Thank you for your literature suggestions; we put these works in our introduction:
“The effect of large-scale PV anomalies accompanied by cut-off lows on deep moist convection (in relation to severe precipitation events) has already been observed in other studies showing for Europe that this is an important mechanism for convection due to the associated patterns of advection and vertical motion (Roberts, 2000; Morcrette et al., 2007; Browning et al., 2007; Russell et al., 2012). But the effect is complex and not well understood.”

p.3, line 62: "A connection between atmospheric blocking and heavy precipitation events..." - Why again blocking? The sentence is almost identical to that on page 2, lines 49-50. Why don’t you merge these parts?
AC: We fundamentally revised the introduction and considered (or rewrote) this point.
“At first, the relationship between atmospheric blocking and severe convection seems counterintuitive because heat-waves and associated droughts are frequently associated with such patterns (e.g., Pfahl and Wernli, 2012a; Bieli et al.,752015; Schaller et al., 2018; Röthlisberger and Martius, 2019). But in peripheral locations upstream and downstream blocks can also create environmental conditions conducive for deep moist convection development. For example, the link to heavy precipitation events (including flood events) has already been established in the last decade (e.g., Martius et al., 2013; Grams et al., 2014; Piaget et al., 2015; Sousa et al., 2017; Lenggenhager et al., 2018; Lenggenhager and Martius, 2019).”

p.3, line 68-70: "[..] such situations are usually associated with weak wind speeds at mid-tropospheric levels (cf. PIP16), so that thunderstorms become almost stationary and usually do not develop into organized structures such as large mesoscale convective systems or supercells." – First: where is the wind weak? in the high, the low, at the western flanks?
AC: Over the area, where we observed / investigated the thunderstorms.
Second: What about HP-supercells (high precipitation supercells)? Can you please comment on HP-supercells.
AC: HP-supercells might have occurred. As we haven’t investigated that, we rewrote the sentence “In addition, such situations are usually associated with weak wind speed at mid-tropospheric levels and thus weak vertical wind shear over the thunderstorm area with the consequence that thunderstorms become often stationary and rarely develop into large organized convective systems.”

p.3, line 83: What do you mean with "secondary effects"? Please elaborate.
AC: We mean their sub-perils (e.g., hail, heavy rain, wind gusts); we added an explanation:
“thunderstorms and secondary effects such as heavy rain, hail and convective wind gusts”

p.3, line 85: "(May/June)" - These are the whole months (1.5-30.6)? It is confusing since you already stated two different periods in the text before.
AC: Yes, the whole month; we added this information (1 May to 30 June).

p.4, line 87-93: Please clarify what the purpose of the ESWD data is. Do you use different quality levels or all? Why don't you show the reports also in e.g. Belgium or Italy?
AC: The purpose of the ESWD data is to show the sub-perils associated with the thunderstorms, and that these were preferably heavy rain events. We use all data above QC0+ (we added this).
ESWD Data from Belgium have already been used (see Fig. 2) – since it is in our study area. Maybe you mean the precipitation data from Belgium (here we were not able to get any). Data from Italy are not included because Italy is not included in our study area (see lines 92-93 "The study area includes parts of central and western Europe - France, Benelux (Belgium, Netherlands, Luxembourg), Germany, Switzerland and Austria (see Fig. 1)" – for which data were available.

p.4, line 88: It is good to know that the ESWD collects data about heavy rain, hail and wind gusts. However, what data did you use for the analysis?
AC: All these three sub-perils. We clarified this.

p.4, line 90: better: "[..] mainly based on reports of storm chasers, [..]"
AC: We corrected this.

p.4, line 108: Is there a description of the REGNIE data in English for non-Germans, too?
AC: Not really, but about HYRAS, which uses the same methodology and which is already cited (Rauthe et al., 2013).

p.4, line 104-111: Why did you decide to use the REGNIE data. The data seems to interpolate measured precipitation on a regular grid. Is the REGNIE data suitable to analyse extreme convective precipitation which might be short in duration and small in scale? Or might these extremes be smoothed during the interpolation process? Did you consider to use a highly-resolved reanalysis data set for comparison reasons?
AC: We used REGNIE data only for the estimation of return periods because of their long-term availability of approx. 70 years, and the large number of approx. 2,000 climate stations used in the regionalization method. RADOLAN data (merger between Radar and station data) would be a better choice, but are available only for 20 years and, thus, not suitable to estimate return periods. Reanalysis also tend to underestimate precipitation totals. We included an explanation on this.

p.4, line 109-111: "Note that the REGNIE time series are affected by temporal changes in the number of rain gauges considered by the regionalization. For our purpose, the homogeneity of the data are sufficient." - Can you please give a reference here? Did the number of stations change in the analysed period?
AC: We included the reference Rauthe et al. (2013). Unfortunately, there is no recent reference available; also the exact number of stations for the regionalization is not known (it was approx. 2,000 stations in 2011).

p.4, line 115: "[..] appropriate for precipitation statistics [..]" - can you please give a reference here and explain a bit more in detail what was done in the previous literature with the Gumbel distribution.
AC: That's right, "precipitation statistics" is a little too generic. We changed this sentence into: "The Fisher-Tippett Type I distribution, also known as the Gumbel distribution (Gumbel, 1958; Wilks, 2006), has been extensively used in various fields including hydrology for modelling extreme events, i.e. to estimate statistical return periods or return values (Sivapalan and Blöschl, 1998; Rasmussen and Gautam, 2003). The Gumbel cumulative distribution function (CDF) is given by:"

p.4, line 112-123: General comment: Is this method new? If so, please state here, otherwise, please write something like: "we follow the methodology used in..."
AC: No, is not new. We clarified this.

p.4, line 116: R is not explained.
AC: That's correct. We added this (R is the investigated variable, here precipitation values.)

p.5, line 117: Can you please give a reference for the "Method of Moments". If it is also explained in the Wilks-book, maybe you can add the chapter to the reference here.
AC: Yes; it is explained in Wilks (2006) in Chapter 4 (Parametric Probability Distributions).

p.5, chapter 2.1.3: What will you use the data for?
AC: (Note now chapter 2.1.1) "Lightning data offer the best spatially homogeneous coverage for a full thunderstorm detection, but does not distinguish according to the severity. For this purpose, we use eyewitness reports of the European Severe Weather Database and precipitation observation (station-based and gridded-based)". Furthermore, the lightning data are used to compare these with the PV cut-offs/filaments. We added this information.

p.5, line 132: what parameters will be taken into account to estimate the "atmospheric conditions"?
AC: As already mentioned the SLI; the second is the V500. We added a comment on this to clarify.

p.5/6, chapter 2.1.5: Can you conclude from the radar data, if the thunderstorms rotated? For example by comparing the direction of the mean tracks to the investigated severe thunderstorms?
AC: For proper detection of rotation in radar data you need the Dual-Doppler wind fields, which we do not have. And even with that the detection or rotation is very difficult (we didn't even detect rotation in the radar data of the severe supercell on 28 July 2013; cf. Kunz et al., 2018). Because the track direction depends – in addition to vertical pressure disturbances - on various effects such as the vertical extent of the cells relative to the wind shear or the formation of new cells (particularly in case of multicells), a comparison between the two as suggested would not allow to give any conclusions about the rotation of the cells.
Kunz, M., Blahak, U., Handwerker, J., Schmidberger, M., Punge, H. J., Mohr, S., Fluck, E., and Bedka, K. M.: The severe hailstorm in SW Germany on 28 July 2013: Characteristics, impacts, and meteorological conditions, Q. J. R. Meteorol. Soc., 144, 231–250, https://doi.org/10.1002/qj.3197, 2018.

p.6., chapter 2.2: What fields will you use?
AC: See Lines 193-195: "Beside the atmospheric stability (based on SLI), we examine in the study V500, the bulk wind shear (BWS; e.g., Thompson et al., 2007), 500 hPa geopotential height (Z500) and the vertically integrated water vapor (IWV)."

p.6, line 172/173: "[..] but reflects important seasonal differences." - What do you mean here?
AC: Classical weather regime definitions typically distinguish summer and winter regimes. Our year-round definition contains these seasonal different patterns and therefore has more regimes than classical definitions. Still these patterns can occur in any season and are important for local weather conditions.
A figure showing the weather regimes would be nice, at least later in the text, where you analyse the data, you could show the typical patterns of the prevailing regimes.
AC: The illustration of the Atlantic-European weather regimes can be found in Grams et al., 2017 – however in the Supplementary information (Supplementary Figure 1); but only for the winter season, but which are very similar to the summer season. We now provided the typical patterns (for May/June) as supplementary material (see Supplementary Figure 1).

p.7, chapter 2.4: Is this method new or does it already exist? Please clarify.
AC: Similar approaches have been used to relate surface weather to weather objects in earlier work (e.g., Pfahl and Wernli 2012, 2014; Pfahl et al. 2014). We now clarified this in the text.
Still as far as we know this is the first study matching lightning data to cut-off cyclones.

p.7, line 197: general comment: The Brunt-Vaisala frequency is smaller in summer, too, due to decreased stability.
AC: Here we aim to provide a physical justification for the scale of our buffer radius not an exact estimation which would depend on each specific case. We think our scale analysis yields a reasonable estimate of a remote influence and that seasonal variation in stability would not change the order of magnitude. In addition, we tested the sensitivity to a range of buffer radii with now impact on our qualitative interpretation.

p.7, line 199-203: You could add a table to the supplementary material showing the change in associated lightning.
AC: We included a table in the supplementary materials (and also the results/Fig. for a buffer radius of 400 km and 600 km).
As stated in the main text, the buffer radius of 500 km is chosen subjectively. We know that there is an uncertainty involved but that a radius below 400 km or above 600 km is not appropriate from a meteorological perspective. Changing the buffer Radius to 400 or 600 km yields the following conclusions:
1.) The percentage of lightning strikes that can be linked to a cut-off low does not change in the first five days of the study period. This is due to the fact that only a few cut-off lows were identified at that point.
2.) The percentage of lightning strikes that are matched with cut-off lows changes in the most active period from 27 May to 1 June. For a radius of 400 km 60 % of the lightning data can be matched, for 500 km 75 % and for 600 km 88 %. This shows that there is a relatively high sensitivity for this main area to the chosen radius. Following our arguments in the paper, we believe that 500 km is a conservative radius and 600 km are probably even more appropriate. This can also be seen in the overview plots for the period from 31 May to 1 June with the buffer radius (see supplementary). Moreover, even with a low radius of 400 km more than half of all the lightning strikes in this most active period can be linked to a cut-off low.
3.) The overall matched lightning percentage increases from 42.2 % to 64.3 %, which shows that there is a sensitivity to the chosen radius but that these results do not change our conclusions.
Moreover, it would be nice to see this "buffer zone" in the figures.
AC: We decided not to include a figure including the buffer zone in the main text (otherwise it would be too obvious), but we included it in the supplement for the interested reader.

p.8, line 211-214: Why do you use the wind speed at 500hPa instead of the deep-layer shear? Additionally, deep-layer shear is a widely used variable and the results would be better comparable to the existing literature. I do not understand the motivation here, especially since the authors later in the paper discuss the importance of shear on the organization of thunderstorms.
AC: We made a conscious decision to show V500 and not the shear (although we had already examined both). One reason for V500 was the connection with the propagation speed of the cells (see also the comment on propagation speed below), since our focus in the work was not to analyse the organizational structure of the cells using wind shear. Furthermore, the interesting point for us was the really extraordinary low wind speeds in the mid-troposphere.
In the panel of Figure 7 we now additionally included the bulk wind shear between 10 m and 500 hPa – showing that the values averaged over the study period are almost similar to V500. We added also a comment on that (Lines 403-408).

p.8, line 216: "Overview" - Can you please be more precise, there is another chapter which is also called overview. What is you intention of this whole chapter?
AC: We restructured the headings in Chapter 3.

p.8, line 222/223: "The three-week period from 22 May until 12 June was the most active thunderstorm episode with a total of 868 heavy rain, 144 hail, and 145 convective wind gust reports based on the ESWD." - do you mean "the most active thunderstorm episode" in the year 2018 or inother period?
AC: During our extended study period (1 May to 20 June) or also in May / June 2018. We clarified this point.

p.8, line 223/224: "An average area of 715,000 km2 was affected by lightning per day" - is that much, what is the average value for Europe?
AC: Yes, this is twice the area of Germany per day, that's much! We included the relation to the area of Germany.

p.8, line 227/228: "As shown in Figure 2b, most of the severe weather reports came from the western part of France, Benelux, central and southern Germany, and the easternmost part of Austria." - Can you explain the gap in central/eastern France? From your Fig. 8 Lifted index was negative, too. Moreover, the mean wind was not much different from western France?

AC: This primarily depend on the availability of storm chasers, eyewitnesses, or voluntary observers. We added a comment on this: “While the spatial composition of the ESWD reports shows regional gaps due to an under-representation of eyewitness reports, for example, in Central and south-eastern France (cf. Groenemeijer et al., 2017; Kunz et al., 2020), thunderstorm days are observed throughout the study area”. We included a thunderstorm day map of the study period in the Supplement (SFig.2).

p. 8, line 241: Isn’t the number of ESWD reports depending on the number of people reporting events? Is there a difference if you just use some of the quality levels?
AC: Right. And the quality levels can't fix this. The reports in the ESWD are absolutely controlled by the activity of the different people. Here, the population density plays a significant role or where the most active "reporters" live and what their area of investigation is. There are very severe events, which have smaller number of reports that less severe events.

p.9, line 252: "low wind speed [..] slow propagation" - You could mention here, that you will give more details later in the text. While first reading through the text, I wondered if these statements will be verified later or just stated as a fact here?
AC: Note that the Section 3 (Part 1) is completely revised. We followed the suggestion and added a reference and further comment on that (now Lines 287-297; text passage with tracking/propagation speed was moved).

p.9, line 257: What is meant with "The strength and spatial extent of the lifting forcing varied from day to day, [..]"? Can we see this in one of the figures?
AC: We deleted the sentence.

p.9, line 260-273: Just write about the events that are explained in more detail. All other numbers will just lead to confusion and can be seen in the table.
AC: Ok, we followed the suggestion. The Section 3 (Part 1) is completely revised (and was shortened).

p.10, chapter 3.3: It would be reader-friendly if you explained what the intention of this chapter is. Please give an introductory sentence.
AC: We included a more detailed description at the end of the introduction, so this should help the reader for the storyline. Additionally, we included a sentence at the beginning of Section (now) 3.1 for the storyline.

p.10, lines 292-303: It would be a helpful addition if you overlayed the ESWD data. This would make it easier to follow your arguments.
AC: We implemented the suggestion. Note, however, that the first four days of the panel are even days on which no ESWD reports were reported (cf. Fig. 2).

p.11, lines 312-313: Can you please plot the typical patterns of the Zonal regime and the European Blocking.
AC: The illustration of the Atlantic-European weather regimes can be found in Grams et al., 2017 – however in the Supplementary information (Supplementary Figure 1); but only for the winter season.
We now provided the typical patterns (for the May/June season) as supplementary material.

p.11, lines 315-323/line 330: Can you plot in Fig 6/7a+b additionally to the regimes/sounding data, the lightning activity (out of Fig. 2a) for easier comparisons.
AC: We did not integrate the lightning data into the two figures, which made it too confusing. Instead, we combined the two figures and noted that the vertical black bars represent the study period, which was the period with the highest lightning activity (see Fig. 2).

p.12, line 348/349: "Because of the low wind speed in the mid-troposphere, most of the thunderstorms moved very slowly or even became stationary." - The motion of thunderstorms is not necessarily determined by the wind at 500 hPa - can you please give a reference that shows that the storm motion correlates with 500hPa winds.
AC: It’s right, the propagation of convective cells is driven by various factors such as gust-front lifting in case of multicells and vertical pressure gradients extending over a deep layer in case of supercells. We took the 500 hPa wind as a proxy because proper determination of the vertical extent – even though possible – would be

out of the context of this paper. We have overworked and extended the whole paragraph, included to references and moved it into Section 3 (Description of the thunderstorm episode 2018).

p. 12, lines 358-360: "The fact that relatively high PV cut-off frequencies expand over a larger region of western Europe underlines that multiple individual PV cut-offs form on the upstream flank of the blocking ridge, and intermittently move across Iberia, France, the British Isles, the North Sea, and Germany [..]" - How do you distinguish between a stationary cut-off low and newly-formed moving ones in Fig. 10? Please clarify.
AC: We concur that this statement was misunderstandable. We here only refer in the first half of the sentence to Fig. 10 (now reference included after "… western Europe (Fig. 10) underlines that …". The occurrence of multiple cut-offs was explained in the synoptic overview Fig. 4. The references "(see Fig. 4)" is now earlier in the sentence "…of the blocking ridge (see Fig. 4), and intermittently …"

p. 13, line 396: better: " To estimate the severity of the rainfall with respect to the rainfall climatology, [..]"
AC: We changed this.

p. 13/14, chapter 5.1: I wonder if the return periods are dependent on the REGNIE data and how it is designed. Is it possible to get higher precipitation amounts than observed at the stations? Can you please comment on this?
AC: Yes of course, all extreme value estimates depend upon the used data set. REGNIE certainly underestimate the precipitation peaks, but this is the case for both the observation period and the 67-years reference period. We added a comment in this section and a further comment in the data description.

p. 14, chapter 5.2: If I understand it correctly, the only thing one can directly compare in Fig. 14 - left vs. right boxes-and-whiskers - is the median on the left with the complete box-and-whiskers on the right? Maybe you could add the median of the actual period as an extra symbol to the right box-and whiskers.
AC: We decided against this proposal, because we do not want to overload the plot unnecessarily with symbols, which is already very voluminous. In addition, the two box-and-whiskers are very close together, so they are easy to compare. However, we added a comment in the figure caption, which should help.

p. 14/15, lines 435-448: Although, your main intention is presumably, that the investigated storm period is a rare event. From your text, I could not understand how Fig. 15 was produced. Can you please rewrite the text passage and clarify.
AC: We rewrote the description and hope that it is now more understandable and less confusing.
What is meant by skip days and why do you use 3 instead of 1 as in the referenced paper? Please explain.
AC: "Within a cluster of seven event days, we allow one day to be a non-event one (skip day), which is not considered in the total length n. For example, clusters with a length of up to 7 (14/21) days may contain at most 1 skip day (2/3 skip days)." Means one skip day per (started) week.

p. 15, lines: 463-466: "A further relevant condition for the evolution of deep moist convection is the vertical wind shear or, more generally, the wind at mid-tropospheric levels, which is decisive not only for the organizational form, the longevity and thus the severity of the convective storms (e.g., Weisman and Klemp, 1982; Thompson et al., 2007; Dennis and Kumjian, 2017), but also for their propagation (Corfidi, 2003)." - As far as I know, all the cited papers talk about the vertical wind shear, but not about the wind at mid-tropospheric levels (although they might mention storm-relative winds, but this can be quite different from the mid-tropospheric wind). Of course, I can be mistaken, hence, please cite the text passages of the papers, where the mid-tropospheric wind is mentioned in your authors's response.
AC: In the panel of Figure 7 we additionally included bulk wind shear between 10 m and 500 hPa. The values averaged over the study period are almost similar to V500. We added a further paragraph that briefly discusses this issue. Furthermore, we deleted wind speed in the quoted sentence.

p. 16, lines 475/476: "[..] air masses were trapped [..]" - Is it possible to show, that the air masses were trapped over several weeks (e.g. by using trajectories)?

AC: Good suggestion; we implemented a Lagrange-based analysis of the air masses, which supports this statement (new Section 3.2 and Figure 9).

p. 16, lines 484-485: "In our investigated case, thunderstorms were often triggered by large-scale lifting associated with upper-level cut-off lows or filaments of high PV that separate from the main PV cut-off" – I am convinced that the cut-off lows provided good environmental conditions for convection, however I doubt that the cut-off lows triggered the thunderstorms directly. What about (older) outflow boundaries? Can you please comment on that?
AC: That's correct. Thunderstorms are triggered by a variety of mechanisms. Large-scale uplift by itself won't bring air-packets up to LFC height, speeds are too low (resp. time scales would be too long for that). Rather, it is the decrease in CIN and the increase in CAPE that are relevant here.
We reformulated this sentence and changed the statements of thunderstorm triggering by large-scale lifting throughout the manuscript.

p. 16, lines 490-496: Especially since the precipitation amounts are so high, how do you know that the thunderstorms were mainly single cells? Moreover, did you mention at any point in your paper, how you differentiate between single cells and other convective thunderstorm types like multicells? Maybe you can put the radar movies for one of the extreme cases you talked about to the supplemental material?
AC: We followed the suggestion and included radar movies for two days (the most severe ones) in the supplementary. These animations show how both single cells and multicells develop throughout the day. A brief discussion is included in Section 3. Furthermore, we weakened the statement about single cells and changed the wording into isolated cells (which clearly can be seen in the radar animations). Finally, we added some more information about the dimensions of the storms detected by the tracking algorithm to Table 1.

Figures:

Fig. 2b: Please do not use the rainbow color scale. It is hard to differentiate between some days. Maybe if you switch to a scale, it might be possible to see some temporal clustering?
AC: We tested different (sequential) colorbars. However, we had to find out that the one used so far is the most suitable one. With a sequential colorbars the available color spectrum is too small to divide the days decently. Furthermore, there was no clear clustering on a time scale of several days, so that the added value of the figure is to be able to identify individual days more precisely (see figure below)..

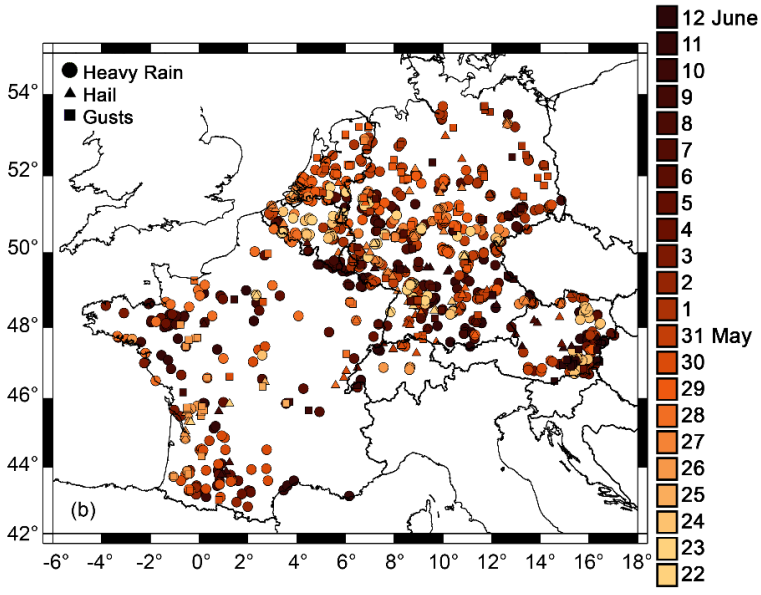

Are there really no events in northern Italy, the Czech republic or Poland?
AC: Data from Northern Italy, the Czech republic or Poland are not included because these are not part of our study area (homogeneity reasons).

Fig. 3b: I cannot see any difference between the blue colors here.
AC: We modified the colorbar.

Fig. 4: Is it possible to add the locations of the ESWD reports of the associated day to maps?
AC: We implemented the suggestion. Note, however, that the first four days of the panel are even days on which no ESWD reports were reported (cf. Fig. 2).

Fig. 6: It is impossible to differentiate between ZO/SCTr, EuBL/SCBL and AT/GL.
AC: We modified the colorbar.
Can you add the affected lightning area (from Fig 2a) to the curves.
Fig. 7: Is it possible to add the lightning data from Fig 2a?
AC: We did not integrate the lightning data into the two figures, which made it too confusing. Instead, we combined the two figures and noted that the vertical black bars represent the study period, which was the period with the highest lightning activity (see Fig. 2).

Fig. 12: There is no red hatching (in my print it looks black?).
AC: Oh, sorry in an older version of the Figure the PV on the 325 K isentropic surface was red. Thanks, we changed this.
Is it possible to add the buffer zone?
We decided not to include a figure including the buffer zone in the main text (otherwise it would be too obvious), but we included it in the supplement for the interested reader.

Fig. 14: Can you please add the median from the left box-and-whiskers as an extra symbol to the right ones?
AC: We decided against this proposal, because we do not want to overload the plot unnecessarily with symbols, which is already very voluminous. In addition, the two box-and-whiskers are very close together, so they are easy to compare. However, we added a comment in the figure caption, which should help.
Please also plot the deep-layer shear.
AC: We decided to include the aspect with the shear in Fig. 7. Since the results are always quite similar (V500 vs. shear; see comment above) or the core statements are not significantly influenced by the result of the shear, we decided against showing the shear for the rest of the figure with V500, since we did not see any added value.

The role of large-scale dynamics in an exceptional sequence of severe thunderstorms in Europe May/June 2018

Susanna Mohr[1], Jannik Wilhelm[1], Jan Wandel[1], Michael Kunz[1,2], Raphael Portmann[3], Heinz Jürgen Punge[1], Manuel Schmidberger[1], Julian F. Quinting[1], and Christian M. Grams[1]

[1]Karlsruhe Institute of Technology (KIT), Institute of Meteorology and Climate Research (IMK), Karlsruhe, Germany
[2]Center for Disaster Management and Risk Reduction Technology (CEDIM), Karlsruhe, Germany
[3]Institute for Atmospheric and Climate Science, ETH Zurich, Switzerland

Correspondence: Susanna Mohr (mohr@kit.edu)

Abstract. Over three weeks in May and June 2018, an exceptionally large number of thunderstorms hit vast parts of western and central Europe, causing precipitation of up to **80 mm in one hour** and several flash floods. During this time, the large-scale atmospheric circulation, which was characterized by a blocking situation over northern Europe, influenced atmospheric conditions relevant for thunderstorm development. Initially, the southwesterly flow on the western flank of the blocking anticyclone induced the advection of warm, moist, and unstably stratified air masses. Due to a low-pressure gradient associated with the blocking anticyclone, these air masses were trapped in western and central Europe, remained almost stationary and prevented a significant air mass exchange. In addition, the low-pressure gradient led **predominantly** to weak flow conditions in the mid-troposphere and thus to low vertical wind shear that prevented thunderstorms from developing into severe organized systems. ~~Most of the storms formed as local-scale, relatively slow-moving single cells. However,~~ Due to the weak propagation speed **in combination with high rain rates**, several thunderstorms were able to produce torrential heavy rain that affected local-scale areas and triggered several flash floods.

Atmospheric blocking also increased the upper-level cut-off low frequency on its upstream regions, which was up to 10 times higher than the climatological mean. Together with filaments of positive potential vorticity (PV), **the cut-offs provided the meso-scale setting for the development of a large number of thunderstorms.** During the 22-day study period, we found that more than 50 % of lightning strikes can be linked to a nearby cut-off low or PV filament. The exceptional persistence of low stability combined with weak wind speed in the mid-troposphere over three weeks has not been observed during the past 30 years.

Keywords: Europe, thunderstorms, severe convective storms, heavy rain, flash floods, atmospheric blocking, weather regimes, cut-off lows, potential vorticity

1 Introduction

Historically, the period from May to mid of June 2018 **was** among the most active periods of severe convective storms associated with heavy rain, hail, convective wind gusts and even tornadoes over large parts of western and central Europe **(WetterOnline, 2018a, b, c; DWD, 2018a)**. More than 1,500 reports of hazardous weather events were documented by the European

Severe Weather Database (ESWD; Dotzek et al., 2009). Rainfall totals of up to 90 mm within a few hours caused (pluvial) flash floods in various municipalities. Gust speeds of up to 30 m s^{-1} led to numerous fallen trees and severely damaged buildings. For example, from 26 May to 1 June 2018, thunderstorms caused **insured losses of about 300 million USD and overall losses of about 430 millions USD** according to Munich Re's NatCatSERVICE (Munich Re, 2019). Thus, it was the costliest convective storm event in western Europe that year.

In general, the development of convective storms results from scale interactions of different processes in the atmosphere. It is well known that deep moist convection depends on three necessary but not sufficient ingredients (e.g., Johns and Doswell, 1992; Trapp, 2013): (i) any kind of instability (conditional, latent, potential) over a layer of sufficient depth and (ii) sufficient moisture in the lower troposphere. These requirements are usually controlled by processes on the synoptic scale. The third ingredient is (iii) a suitable lifting mechanism for the triggering of convection, which can occur at different scale ranges. For example, lifting mechanisms on the mesoscale include orographic lifting, horizontal convective rolls, or gravity waves (e.g., Wilson and Schreiber, 1986; Browning et al., 2007; Barthlott et al., 2010), whereas large-scale lifting can be related to drylines or cold fronts (e.g., Bennett et al., 2006; Kunz et al., 2020). A further relevant condition for the evolution of deep moist convection is the vertical wind shear, which is decisive not only for the organizational form, the longevity and thus the severity of the convective storms (e.g., Weisman and Klemp, 1982; Thompson et al., 2007; Dennis and Kumjian, 2017), but also for their propagation (Corfidi, 2003).

~~Several authors have found a relation between thunderstorm probability and various teleconnection patterns ((e.g., North Atlantic Oscillation, Madden-Julian Oscillation, El Niño-Southern Oscillation; Giaiotti et al., 2003; Barrett and Gensini, 2013; Allen and Karoly, 2014; Allen et al., 2015; Piper et al., 2019). All these mechanisms may operate individually or in tandem, and may directly trigger convection if they are strong enough or — in addition to the daily temperature cycle — serve to precondition of the thermodynamic environment.~~

The general synoptic situation during the thunderstorm episode **2018 investigated in this study** was similar to that prevailing over a 15-day period in May/June 2016, where also an exceptionally large number of thunderstorms caused several flash floods, primarily in Germany **(Piper et al., 2016; Bronstert et al., 2018; Ozturk et al., 2018). During the episode in 2016,** a blocking anticyclone over the North Sea and Scandinavian region prevented an exchange of the dominant unstably stratified air masses over several days. In addition, low wind speeds throughout the troposphere caused the thunderstorms to be almost stationary with the effect of torrential rain accumulations in several small regions (Piper et al., 2016, hereinafter referred to as PIP16).

Atmospheric blocking, with a typical lifetime of several days to weeks, is a quasi-stationary, persistent flow situation that modulates the large-scale extratropical circulation (Rex, 1950a, b; Barriopedro et al., 2006; Woollings et al., 2018). **Such blocks typically occur either in a *dipole configuration* with an accompanying cut-off low on the equatorward side (Rex, 1950a; Tibaldi and Molteni, 1990) or they adopt an *omega-shape* with cut-off lows forming at the flanks of the blocked region (Dole and Gordon, 1983). In the potential vorticity (PV) framework, a cut-off low is an upper-level closed anomaly of stratospheric high PV air (e.g., Wernli and Sprenger, 2007; Nieto et al., 2007a, 2008).** PV anomalies, in general, have a far-field impact on the meteorological conditions in their surroundings (cf. Hoskins et al., 1985). Below the positive PV anomaly, isentropes bend upward, resulting in reduced static stability and increased lifting. Due to an induced cyclonic circulation

anomaly, the positive PV anomaly favours isentropic gliding up and thus ascent along the isentropes that usually bend upward towards the pole. Finally, when the positive PV anomaly propagates, air masses ascend isentropically at the PV anomalies' upstream side. These three mechanisms associated with lifting are intrinsic to upper-level positive PV anomalies in general. Additionally, at the flanks of a mature PV cut-off, small meso-scale filaments of positive PV often separate and are advected away, particularly when the PV cut-off gradually decays (Portmann et al., 2018). When such a positive PV filament moves over air masses that are conditionally or potentially unstably stratified, they trigger lifting and thereby **release – if the air parcel reaches its level of free convection – convective available potential energy (CAPE)** and facilitate/cause deep moist convection (cf. Grams and Blumer, 2015). **The effect of large-scale PV anomalies accompanied by cut-off lows on deep moist convection (in relation to severe precipitation events) has already been observed in other studies showing for Europe that this is an important mechanism for convection due to the associated patterns of advection and vertical motion (Roberts, 2000; Morcrette et al., 2007; Browning et al., 2007; Russell et al., 2012). But the effect is complex and not full understood.**

At first, atmospheric blocking was primarily known for its conjunction to extreme weather events such as cold spells and heatwaves (and associated droughts; e.g., Pfahl and Wernli, 2012a; Bieli et al., 2015; Schaller et al., 2018; Röthlisberger and Martius, 2019). But in peripheral locations upstream and downstream of the blocks can also create environmental conditions conducive for deep moist convection development. Thus, the link to heavy precipitation events (including flood events) has already been intensively investigated in past years (e.g., Martius et al., 2013; Grams et al., 2014; Piaget et al., 2015; Sousa et al., 2017; Lenggenhager et al., 2018; Lenggenhager and Martius, 2019). A new study by Mohr et al. (2019) now shows a statistical relationship between convective activity (based on lightning data) and specific blocking situations in the European sector. They found a block over the Baltic Sea frequently associated with increased thunderstorm occurrences because of southwesterly advection of warm, moist and unstable air masses on its western flank. In addition, such situations are usually associated with weak wind speed at mid-tropospheric levels and thus weak vertical wind shear over the thunderstorm area with the consequence that thunderstorms become often stationary and rarely develop into large organized convective systems. Recently, Tarabukina et al. (2019) also demonstrate a correlation between the annual variation of summer lightning activity in Yakutia (Russia) and the frequency of atmospheric blocking in Western Siberia.

The primary objective of this paper is to examine the conditions and processes that made this particular thunderstorm episode **in 2018** unique. We focus on the process interaction across scales, i.e., from the large-scale dynamics such as atmospheric blocking **to meso-scale PV cut-off lows and/or small meso-scale** PV filaments to modifications of the convective environment to local-scale thunderstorm occurrences. Further objectives are to highlight the synoptic setting during the thunderstorm episode, to demonstrate the severity of the events, and to place the event in a historical context.

The paper is structured as follows: Section 2 presents the different data sets and the methods used. Section 3 **starts with a description of the thunderstorm episode in 2018 and their accompanying phenomena by investigating different observation data such as lightning information, hazardous storm reports, rain gauge measurements, and radar-based storm tracks estimating the propagation speed. Subsequently, the synoptic situation prior and during the examined thunder-**

storm episode is investigated by analyses of the large-scale flow situation, backward trajectories, accompanied weather regimes, and environmental conditions such as instability, moisture, or mid-tropospheric wind speed). Furthermore, we examine the role of PV cut-off and PV filaments on the development of deep moist convection. The next Section 4 puts the results in a historical context, whereby the exceptional nature of the thunderstorm episode is assessed by relating the observed rainfall totals, the prevailing environmental conditions, and the occurrence of cut-off systems to long-term data records. Finally, Section 5 and Section 6 discuss and summarize the main results and draw conclusions.

2 Data and methods

The study area includes parts of central and western Europe – France, Benelux (Belgium, Netherlands, Luxembourg), Germany, Switzerland and Austria (see Fig. 1) ~~– for which data were available~~. The study period extends over three weeks from 22 May to 12 June 2018, where most of the thunderstorms and secondary effects **such as heavy rain, hail and convective wind gusts** occurred (see Sect. 3). **To highlight the synoptic situation prior to the episode and to emphasise that severe convection during the study period was embedded in a longer lasting unusual large-scale flow situation**, we considered an extended study period from 1 May to 20 June 2018. For the purpose of climatological comparison, the 30-year period from 1981 to 2010 (**1 May to 30 June**) was the reference period (unless otherwise indicated).

2.1 Observation data

For the description of the thunderstorm episode in 2018, we use different observation data. Lightning data offer the best spatially homogeneous coverage for a full thunderstorm detection, but does not distinguish according to severity. For this purpose, we use eyewitness reports of the ESWD and precipitation observation (station-based and gridded-based). Radar-based storm tracks allow to investigate the propagation speed of the convective cells. Some investigation are limited to Germany, for which data were available (storm tracks, REGNIE), but enable a deeper insight into the exceptional nature of the phenomenon. Additionally, the atmospheric conditions are examined with data from various sounding stations. Some data are also available consistently and homogeneously over long-term periods, which allow us to compare the episode with historical conditions/events.

2.1.1 Lightning data

Lightning data are obtained from the ground-based low-frequency lightning detection system of Siemens part of the EUCLID network (EUropean Cooperation for LIghtning Detection; Drüe et al., 2007; Schulz et al., 2016; Poelman et al., 2016). Available for the whole study domain, the data are projected on an equidistant grid of $10 \times 10\,\mathrm{km}^2$ and accumulated over 6-hour periods centered around the times in ERA-Interim (e.g., for the 06 UTC reanalysis the lightning period is 03 – 09 UTC). **This allows the data to be linked to the cut-off lows (see Sect. 2.5).** We consider all types of flashes including cloud-to-ground, cloud-to-cloud, and intra-cloud flashes, whereas polarity or peak current are not investigated.

2.1.2 ESWD reports

We use reports of heavy rain, hail (diameter $\geqslant 2$ cm), and convective wind gusts $\geqslant 25\,\mathrm{m\,s^{-1}}$ from the European Severe Weather Database (ESWD; Dotzek et al., 2009; Groenemeijer et al., 2017). The ESWD is a step-by-step quality controlled (four levels) database providing detailed information about severe convective storms in Europe, mainly **based on reports from storm chasers, eyewitnesses, voluntary observers, meteorological services, and news media. We consider all records with a quality level above QC0+**. Using a homogeneous data format, these observations contain information about hazardous weather events such as location, time, intensity, and damage-related information. For a detailed description of the event reporting criteria see ESSL (2014).

2.1.3 Rainfall totals

Daily **rainfall totals** of 232 stations distributed across the domain (41°N – 58°N 4°W – 20°E) were collected from the European Climate Assessment and Dataset (ECA&D), a database of daily meteorological station observations across Europe (Klein Tank et al., 2002). In addition, hourly and daily data were obtained from the Météo-France **(1223/1935 stations with hourly/daily data)**, the Royal Netherlands Meteorological Institute (KNMI; 50/322), the German Weather Service (DWD; 958/810), MeteoSwiss (952/0), and the Central Institution for Meteorology and Geodynamics (ZMAG; 254/0)~~— the national weather services of those countries with the highest count of flash flood reports (see Fig. 1)~~. For statistics of hourly and 3-hour extreme rainfall events, we applied the same severity thresholds used in the ESWD (ESSL, 2014), which amount to 35 and 60 mm, respectively (Wussow, 1922; Nachtnebel, 2003). Note that the 24-hour criterion of 170 mm was not measured at any of the stations.

Statistical return periods of single heavy precipitation events are estimated using regionalized precipitation data (*REGionalisierte NIEderschläge*, REGNIE) provided by DWD (DWD, 2018b). REGNIE is a gridded data set of 24-hour totals (from 06 UTC to 06 UTC on the next day) based on approximately 2,000 climate stations more or less evenly distributed across Germany (the so-called RR collective). The REGNIE algorithm interpolates the measurement data to a regular grid of 1 $\mathrm{km^2}$ considering altitude, exposure, and climatology (Rauthe et al., 2013). **The data covering only Germany are available since 1951. The long-term availability of REGNIE over almost 70 years is the decisive advantage compared to other data sets such as RADOLAN (merger between radar and station data; DWD, 2019), which have a higher spatial and temporal resolution but are only available for 20 years.** Note that the REGNIE time series are affected by temporal changes in the number of rain gauges considered by the regionalization **(Rauthe et al., 2013)**. For our purpose, the homogeneity of the data are sufficient.

Statistical return periods of REGNIE totals are quantified using the Generalized Extreme Value (GEV) distribution (e.g., van den Besselaar et al., 2013; Ehmele and Kunz, 2019). The Fisher-Tippett Type I distribution, also known as the Gumbel distribution **(Gumbel, 1958; Wilks, 2006), has been extensively used in various fields including hydrology for modelling extreme events, i.e. to estimate statistical return periods or return values (Sivapalan and Blöschl, 1998; Rasmussen and**

Gautam, 2003). The Gumbel cumulative distribution function (CDF) for the precipitation totals R is given by:

$$F(R) = \exp\left[-\exp\left(\frac{\zeta - R}{\beta}\right)\right], \tag{1}$$

with ζ and β as location and scale parameters. For their estimation, we use the Method of Moments (Wilks, 2006, Chap. 4) and considered the 67-year period from 1951 to 2017 (summer half-year from April to September):

$$\beta = \frac{\sigma\sqrt{6}}{\pi} \qquad \& \qquad \zeta = \bar{R} - \delta \cdot \beta, \tag{2}$$

with σ as the standard derivation, $\bar{R}$ as the mean of the REGNIE sample and δ as the Euler-Mascheroni constant ($\approx .0.5772$). The return period t_{RP} is directly related to the probability of occurrence of the threshold $P(R \geqslant R_{trs}) = t_{RP}^{-1}$ so that the CDF is given by $F(R) = 1 - t_{RP}^{-1}$. The resulting equation to estimate the return period t_{RP} is:

$$t_{RP}(R) = \left[1 - \exp\left(-\exp\left(\frac{\zeta - R}{\beta}\right)\right)\right]^{-1}. \tag{3}$$

2.1.4 Storm tracks computed from radar reflectivity

Storm motion vectors are computed from three-dimensional (3D) radar reflectivity data from the radar network of DWD. The data, which includes 17 radar stations with dual-polarization Doppler radars, are combined and interpolated into a radar composite with a spatial resolution of $1 \times 1\,\mathrm{km}^2$ (Cartesian grid). The temporal resolution of the individual scans is 15 minutes. Radar reflectivity is available on 12 equidistant vertical levels with a distance of 1 km (lowest level is 1 km above ground). For the whole period between 2005 and 2018, which is used to relate the storm motions computed for the investigation period to the climatology (Sect. 4.1), data were stored in six reflectivity classes only. The two highest classes, which are considered here, range from 46 to 55 dBZ and $\geqslant 55$ dBZ.

To identify storm tracks, the cell-tracking algorithm TRACE3D (Handwerker, 2002) was adapted to the DWD radar composite in Cartesian coordinates. Once the algorithm detects a convective cell core, it can be re-detected in the consecutive time steps and merged into an entire cell track. **Storms are defined by having a minimum reflectivity core of 55 dBZ (corresponding to the highest class) and a vertical extent of at least 1 km. Thus, only severe convective storms frequently associated with hazardous weather are considered. Thunderstorms above the 55 dBZ threshold usually form a well-defined core of high reflectivity that can be easily and reliably tracked.** Based on TRACE3D, information about width, length, duration, and propagation speed, as well as direction, is available for each individual thunderstorm track. **Note that we mainly use tracking to estimate the propagation speed and direction of the cells (Sect. 3 and Sect. 4.1). Even if weaker cells are not detected using the 55 dBZ thresholds, it can be assumed that they cannot move at higher speeds.** More details about data and the tracking method can be found in Puskeiler et al. (2016) and Schmidberger (2018). Due to a lack of 3D radar data for France in 2018, our investigation refers only to severe convective storms that occurred in Germany.

2.1.5 Sounding stations

Atmospheric conditions are estimated from vertical profiles of temperature, moisture, **wind speed and direction** at seven sounding stations provided by DWD and the Integrated Global Radiosonde Archive (IGRA) from the National Climatic Data

Center (Durre et al., 2006). These stations are distributed over the entire domain: Bordeaux (44.83°N 0.68°W) and Trappes (48.77°N 2.00°E) in France; Essen (51.41°N 6.97°E), Stuttgart (48.83°N 9.20°E), and Munich (48.24°N 11.55°E) in Germany; Payerne (46.82°N 6.95°E) in Switzerland, and Vienna (48.23°N 16.37°E) in Austria (see Fig. 1). Other sounding stations could not be used because of multiple gaps in the time series.

Atmospheric stability can be estimated, for example, by **CAPE as well as by the surface-based Lifted Index (SLI; Galway, 1956). The latter, which we use in the following, has proven to be as suitable parameter as CAPE for estimating instability in several studies (e.g., Huntrieser et al., 1997; Sánchez et al., 2009; Westermayer et al., 2017; Rädler et al., 2018). There are studies, in which SLI has even shown a better prediction skill than CAPE (e.g., Haklander and van Delden, 2003; Manzato, 2003; Kunz, 2007; Mohr and Kunz, 2013). In addition to the SLI, we also investigate the horizontal wind speed in 500 hPa (V500). Both variables are analysed at 12 UTC, since thunderstorms in central Europe usually peak during the late afternoon (Wapler, 2013; Piper and Kunz, 2017; Enno et al., 2020).**

2.2 Model data

We use the European Centre for Medium-Range Weather Forecasts (ECMWF) high-resolution operational analysis data and ECMWF ERA-Interim reanalysis (Dee et al., 2011) to describe the large-scale meteorological conditions and to calculate weather regimes (see Sect. 2.3), **kinematic backward trajectories (see Sect. 2.4)**, and cut-off lows (see Sect. 2.5). ECMWF analysis is available 6-hourly interpolated to a regular grid with 0.125° horizontal resolution. ERA-Interim used for the historical analysis is available 6-hourly interpolated to a regular grid at 1.0° horizontal resolution. **Beside the atmospheric stability (based on SLI), we examine in the study V500, the bulk wind shear (BWS; directional shear) as wind difference between 10 m and 500 hPa calculated by vector subtraction (e.g., Thompson et al., 2007), 500 hPa geopotential height (Z500) and the vertically integrated water vapor (IWV).**

2.3 North Atlantic-European weather regimes

The large-scale flow conditions in the Atlantic-European region are characterized in terms of a definition of seven year-round weather regimes based on 10-day low-pass-filtered 500 hPa geopotential height anomalies (Z500'; Grams et al., 2017). The regimes are identified by k-means clustering in the phase-space spanned by the seven leading empirical orthogonal functions (EOFs). Based on these seven clusters, an active weather regime life-cycle is derived from the normalized projection of each 6-hourly anomaly in the cluster mean following Michel and Rivière (2011). Thereby, time steps with weak projections are filtered out (no regime). An active regime life-cycle persists for at least 5 days but fulfills further criteria as described in Grams et al. (2017).

Our weather regime definition is in line with 'classical' concepts of four seasonal regimes for Europe (e.g. Vautard, 1990; Michelangeli et al., 1995; Ferranti et al., 2015), but reflects important seasonal differences. Three of the seven regimes are dominated by a negative Z500' and enhanced cyclonic activity **(see Supplementary Fig. 1)**. These are the *Atlantic Trough (AT)* regime with a trough extending towards western Europe, the *Zonal regime (ZO)* with cyclonic activity around Iceland, and the *Scandinavian Trough (ScTr)* regime with a trough shifted towards the east. The remaining four regimes are characterized by a

positive Z500' centered at different locations and therefore referred to as 'blocked regimes'. These are the *Atlantic Ridge (AR)* regime, with a blocking ridge over the eastern North Atlantic and an accompanying trough extending from eastern Europe into the central Mediterranean, the *European Blocking (EuBL)* regime, with a blocking anticyclone extending from Western Europe to the North Sea, *Scandinavian Blocking (ScBL)*, with high-latitude blocking over Scandinavia, and *Greenland Blocking (GL)* with a blocking ridge over the Greenland-Icelandic region.

2.4 Lagrangian Analysis Tool

The path of the air masses during the thunderstorm period from 22 May to 12 June is traced by calculating 10-day kinematic backward trajectories from ERA-Interim using the Lagrangian Analysis Tool (LAGRANTO, Wernli and Davies, 1997; Sprenger and Wernli, 2015). The trajectories are initialised 6-hourly on each day of the study period from the five ERA-Interim grid points surrounding the seven sounding stations (Fig. 1 yellow squares). In order to represent the Lagrangian history of moist, low-tropospheric air masses that contributed to the severe thunderstorms, trajectories are initialised every 50 hPa between 950 and 600 hPa, where the air masses relevant for the thunderstorm development are located.

2.5 Identification of PV cut-off low and matching with lightning data

We identify upper-level cut-off lows based on PV on the 325 K isentropic surface from ERA-Interim using the algorithm of Wernli and Sprenger (2007) and Sprenger et al. (2017). The optimal level for the inspection of weather systems on isentropic surfaces depends on the season. The specific level of 325 K used here is motivated by the literature (cf. Röthlisberger et al., 2018) and the inspection of isentropic PV charts for our case. The algorithm searches for closed areas of PV larger than 2 PVU, which are disconnected from the main PV reservoir that expands across the North Pole.

Following earlier approaches to match weather objects with surface weather (e.g., cyclones and precipitation; Pfahl and Wernli, 2012a, b), the identified PV cut-off lows (including their PV filaments) are then related to thunderstorm events using lightning data on the $10 \times 10\,\mathrm{km}^2$ grid cells. We utilize the smallest distance approach to link a grid cell in the lightning data set to a grid point in the PV cut-off data set. The different grid sizes between the model and observation data sets require matching multiple grid cells (lightning data) to one PV cut-off grid point. This means if a grid point shows the presence of a PV cut-off, all flashes from the associated grid cells are linked to it.

To account for the far-field impact of lifting and destabilization by a PV cut-off, we expand the PV cut-off mask by a buffer. This scale is estimated from the typical Rossby radius of deformation

$$L_R = \frac{N \cdot H}{f_0} \tag{4}$$

associated with a PV cut-off. Here, N is the Brunt-Väisälä frequency, H is the scale height, and f_0 is the Coriolis parameter. For characteristic values in mid-latitudes with $N = 0.01\,\mathrm{s}^{-1}$ and $f_0 = 10^{-4}\,\mathrm{s}^{-1}$, N/f_0 is typically in the order of 100. A scale height of 10 km leads to a Rossby deformation radius of 1,000 km, which is typical for synoptic scales. We assume that some of the PV cut-offs during the study period have a vertical extent of **less** than 10 km. Therefore, we chose a conservative

deformation radius (buffer) of about 500 km. The robustness of the chosen deformation radius is investigated both qualitatively and quantitatively. We found that a change in the radius of 100 km, for example, leads to an increase or decrease of around 10 % in the total amount of lightning strikes associated with a PV cut-off during our study period (see Supplement Sect. 2). Such small changes do not affect the qualitative interpretation of our results.

2.6 Persistence analysis

Days with constant atmospheric conditions tend to form temporal clusters of certain weather events (here thunderstorms) with a lifetime of several days. This behavior can be described statistically by the concept of persistence. The **cluster length or event persistence** n of a specified event is defined as the sequence of days (between 1 and x days) with the binary parameter with values of 1 (event day = criterion fulfilled) or zero (non-event day = criterion not fulfilled). Within a cluster of seven event days, we allow one day to be a non-event one (skip day), which is not considered in the total length n. **For example, clusters with a length of up to 7 (14/21) days may contain at most 1 skip day (2/3 skip days).** For more information on the concept see PIP16.

In the study, we investigate the co-occurrence of low stability (using SLI) and low mid-tropospheric wind speeds (using **V500**). For this purpose, the same thresholds as in PIP16 are chosen, **which were used to investigate the exceptional atmospheric conditions of a similar thunderstorm episode.** We employ the basic criterion, which is fulfilled if both conditions apply: SLI < 0 K and V500 $< 10\,\mathrm{m\,s^{-1}}$ (TH_{BC}). In addition, we also discuss our results in context with the strict criterion, which is fulfilled with SLI < -1.3 K and $\mathrm{v}_{500hPa} < 8\,\mathrm{m\,s^{-1}}$ (TH_{SC}). **Both thresholds were originally determined by choosing the maximum of the daily minima in the case study to capture the prevailing (exceptional) atmospheric conditions.**

3 Description of the thunderstorm episode 2018

The period from **the first of** May to mid-June 2018 was characterized by a large number of thunderstorms that spread across the study area, several of which were associated with heavy rainfall, hail, and strong wind gusts (Fig. 2a). More than 1,500 severe weather reports were collected and archived by the ESWD in our study area during that period. Lightning strikes were recorded on each day, and the affected area ranges between 100 km^2 on 19 June and **1,140,000 km^2 on 27 May** (accumulations of the $10 \times 10\,\mathrm{km}^2$ grids).

The three-week period from 22 May until 12 June was the most active thunderstorm episode **in May/June 2018** with a total of 868 heavy rain, 144 hail, and 145 convective wind gust reports based on the ESWD. **The highest number (152 reports) was issued on 29 May, followed by 31 May (137 reports), most of them reporting heavy rainfall leading to a couple of flash floods and landslides, which destroyed buildings, vehicles, streets and even railway tracks (DWD, 2018a; WetterOnline, 2018b). On average, an area of 758,000 km^2 – an area twice the size of Germany – was affected by lightning per day, with the result that thunderstorms covered the entire study area. As shown in Figure 2b, most of the severe weather reports during the episode came from the western part of France, Benelux, central and southern Germany, and the easternmost part of Austria. While the spatial distribution of the ESWD reports shows several regional gaps due to an**

under-representation of eyewitness reports, for example, in Central and southeastern France (cf. Groenemeijer et al., 2017; Kunz et al., 2020), thunderstorm days are observed throughout the study area (see Supplementary Fig. 4). The extraordinarily large number of thunderstorms, several of them severe, and the unusual persistence of that situation over three weeks motivated us to select that time frame as the study period.

~~As adumbrated in the previous section, heavy rain in May and June, especially during the study period, was a striking phenomenon, chiefly because of the low wind speed and the associated slow propagation of the thunderstorms.~~ **Figure 3 summarizes the evaluation of hourly (1 h) and 3-hour (3 h) rain gauge measurements in the study area** exceeding the ESWD heavy rain criteria of 35 mm and 60 mm, respectively. The 1 h criterion was fulfilled during the study period 167 times (Fig. 3a) and an average of about 7.6 stations per day with a variability between one and 20 stations. **This highest number of stations belongs to** the day with the second most ESWD severe weather reports (**31 May**). The 3 h criterion was reached 38 times, with a maximum of at least 5 stations on three days. ~~The strength and spatial extent of the lifting forcing varied from day to day, which explains the fluctuations of daily heavy rain frequencies.~~ The location of the respective stations shows heavy rain events in all of the countries under consideration without any clustering (Fig. 3b,c).

During the episode, the thunderstorms developed mainly as isolated cells and clusters of several cells, the latter preferably in the early evening and night. Only on a few days (e.g., on 22 May or 1 June) larger mesoscale convective systems (MCS) formed, which persisted during the night and early morning. Animated images of radar reflectivity can be found in the Video Supplement for two representative days: 27 and 31 May. The two animations show a large number of both isolated thunderstorms with a short lifetime of approximately 30 min (radar visibility) and cell clusters persisting over several hours. Most cells moved very slowly or even remained stationary during the two days.

The slow movement of the convective cells, a prominent feature of the entire thunderstorm episode, was mainly due to the low wind speed at mid-tropospheric levels (cf. Sect. 3.1.2). According to the cell tracking (Germany only; see Sect. 2.1.4), about half of all cells reaching a radar reflectivity of at least 55 dBZ had a propagation speed of less than 5 m s^{-1} (47.3 % from 480 cells); only a few cells (1.5 %) had a speed above 15 m s^{-1} (Fig. 4). Mean (standard deviation) and median values are 5.9 m s^{-1} ($\pm$ 2.9 m s^{-1}) and 5.2 m s^{-1}, respectively, which is almost half of the long-term values (cf. Sect. 4.1). The predominant propagation direction was from southeast to northwest (26.3 % of the detected cells). However, several cells moved in completely different directions on the same day – a clear sign that the propagation was not only determined by the (weak) mid-tropospheric wind, but also by internal dynamical effects induced by cold pools or by pressure disturbances (Markowski and Richardson, 2010; Houston and Wilhelmson, 2012). Examples of different track directions of neighbouring cells can be seen in the radar animation on 27 May (14 to 15 UTC, at the coordinates: $x \sim$ 250 km & $y \sim$ 600 km) or on 31 May (21 to 22 UTC; $x \sim$ 400 km & $y \sim$ 700 km).

~~At the beginning of the study period, central Europe was particularly affected.~~ **A detailed look at the chronological sequence during the episode (Fig. 2b) shows that** thunderstorms associated with heavy rainfall and small hail with diameters of around 2 cm were restricted to Benelux and western Germany on 22 May. Some entries report on flash floods and mudslides, for example in the Heilbronn area (SW Germany). Two days later, on 24 May, the federal state of Saxony (east Germany), the east of Austria, and parts of Belgium were hit by torrential rain accumulations. The German station Bad Elster-Sohl in

Saxony (see Fig. 1) on the border to the Czech Republic, for example, measured a record of 86.3 mm / 3 h and 154.9 mm / 24 h. On 26 May, several wind reports with gust speeds of up to 29 m s^{-1} (Poitiers, France; see Fig. 1) and hail reports indicating hailstones with a diameter of up to 5 cm were recorded in the French coastal region of the Bay of Biscay.

The subsequent time frame from 27 May to 1 June was the most active both in terms of the area affected by lightning and the number of ESWD reports (Fig. 2a). Widespread thunderstorms were observed mainly in Benelux, Germany, and France, but also sporadically in Switzerland and Austria, many of them associated with large rain accumulations and subsequent flooding, hail between 2 and 4 cm in diameter, and damaging wind reports. **Many of record-breaking 1 h and 3 h rainfall totals occurred within this period (Table 1). For example, the weather station Bruchweiler (see Fig. 1), located in the west of Germany, measured a 24 h rain accumulation of 145.0 mm on 27 May (Note that the station only provides reports for the full 24 hours). However, this rain amount was fallen within 3 h, while a rain rate of more than 60 mm was observed within 50 min alone (see also Supplementary Fig. 5a). The corresponding track, derived from TRACE3D, has a length of 21 km and a propagation speed of 5.7 m s^{-1} (Table 1). A second example is on 31 May** the conspicuously high 1 h rain accumulation of 85.7 mm measured at Dietenhofen close to Nuremberg in the south of Germany (see also Fig. 3b), listed high in the ranking of highest 3 h rainfall totals as well. **The station was fully hit by an isolated system, which was relatively stationary. The rain rate above 60 mm was present over 35 min (see also Supplementary Fig. 5b and Video Supplement).**

In the first half of June, some hail stones ~~(up to 5 cm)~~ and heavy rainfall were still reported almost daily somewhere in the study domain, though less frequently than before. ~~Also, the area affected by lightning shows a decrease by 2 June.~~ Towards the end of the study period, convective activity increased again. Especially on the last day of the study period, on 12 June, the proportion of gust reports indicating wind speeds between 25 and 31 m s^{-1} to all reports was very large. **After the convectively most active period, when environmental conditions became more stable (cf. Sect. 3.1), thunderstorms rarely occurred. The area affected by lightning decreased considerably and no further severe weather reports were archived in the ESWD.**

As we will show later (Sect. 3.1.2), the wind shear values over the study area were predominantly very low. Individual cases with hail stones of 5 cm were feasible, because close to the border of our study area over the Pyrenees to the east two times regions with high shear (up to 20 m s^{-1}) were advected, which led to the large hail in southwest France (26 May/9 June) or southern Germany (11 June). However, these were exceptional cases.

~~Similarly high 3 h values gauged in Prades-le-Lez in southern France on 11 June, Puchberg am Schneeberg in eastern Austria on 12 June and the above mentioned station Bad Elster-Sohl in eastern Germany on 24 May (see locations in Fig. 1). At the latter station, the extremely high 24 h total of 154.9 mm was caused by a slightly multicellular organized and very slow-moving convective system that was elongated in the propagation direction. Due to that configuration, the station Bad Elster-Sohl was hit successively by several embedded individual cell cores of the entire cluster. Several streets and buildings were flooded and a barrage dam over-flowed.~~

~~One week later, in the evening hours of 31May, a slow northwest-moving multicellular system formed along a convergence zone in northeastern France and southwestern Germany in the evening hours. This day exhibited the highest number of stations (20) with 1 h precipitation accumulations of more than 35 mm (Fig. 3a), appears four times in the top list of 1 h rainfall totals~~

~~in Table 1, and also had more than 110 heavy rain reports in the ESWD (Fig. 2a). Another exceptional example is the last day of the study period, 12 June, where in addition to the high number of gust reports mentioned above, five of the nine highest 24 h rainfall totals occurred (cf. Table 1). In southwestern France and the Alps including its surroundings, continuous rain with regionally strong embedded convection occurred, as more stable air masses poured in the west and central Europe from the northwest.~~

3.1 Synoptic overview

The synoptic situation prior to the thunderstorm episode in 2018 was embedded in a longer lasting unusual large-scale flow situation. At the beginning of the extended study period, a large-scale mid-tropospheric area of high geopotential stretched out from the Azores over central Europe and the Baltic to western Russia (Fig. 5a), attended by a corresponding prolonged lower-level high-pressure system (not shown). This configuration was associated with the advection of warm and relatively dry air masses over large parts of Europe. In the second week of May, the pattern transitioned into a blocked situation over Europe (see Sect. 3.1.1). The geopotential height at 500 hPa depicts the typical *Omega*-like structure with high geopotential over central Scandinavia, flanked by one pronounced trough upstream over the Northern Atlantic and one downstream over Western Russia (Fig. 5b). Subsequently, the two troughs turned into enclosed cut-off lows filled with relatively cold air and finally merged into one system located over central Europe on 15 May (not shown). In the third week of May, the cut-off moved slowly northeastward on an erratic track while gradually dissipating over central and eastern Europe, leaving a moderately warm and dry air mass with weak gradients over central Europe (Fig. 5c).

The study period from 22 May to 12 June was characterized by a rather stationary and persistent synoptic situation with a pronounced blocking ridge stretching from Iceland over the North Sea to Scandinavia and Northeast Europe (Fig. 6a). As a consequence of the synoptic setting during this episode, the mid-tropospheric flow was weak over most parts of Europe (see Sect. 3.1.2). On average, the ridge was flanked by long-wave troughs: one on the western side with the axis pointing from Baffin Bay to Newfoundland, the other on the eastern side stretching from the Barents Sea to Kazakhstan, while the ridge remained relatively stationary centered over the North Sea region (Fig. 5c-f).

A noticeable feature in the mean 500 hPa geopotential height for this episode is a locally enclosed geopotential minimum over the Bay of Biscay and its surroundings (Fig. 6a) that emerges from repeating/transient cut-off lows forming on the upstream side of the blocking ridge. On 25 May (Fig. 5d), a cut-off low (C1a) approached Iberia – which merged in the next days with the cut-off located over the Celtic Sea (C1b) – and triggered several storms, first in France and then in Benelux and Germany (cf. Fig. 2). In the following days, a new cut off (C2; not shown) formed west of Spain, which subsequently influenced the weather there and disappeared relatively quickly. On 1 June, another cut-off (C3) advanced from the Atlantic (Fig. 5e), with some impact on convective activity over France, and then developed into a shallow low-pressure zone in central Europe. Several convergence lines were formed in that zone. In addition, this situation provided very moist air (IWV well above 30 $\mathrm{kg\,m^{-2}}$ over large areas) until 9 June in eastern France and central Europe (Fig. 5e,f). In the end phase of the study period, the next cut-off low (C5) with its associated fronts and convergence lines affected the western half of France and central

and southern Germany and lasted until 12 June (Fig. 5f). Simultaneously, a cut-off (C6) over the British Isles influenced the weather in northern Europe.

The geopotential anomalies at the 500 hPa level, calculated as the deviation from the climatological mean (1981 – 2010), exhibit for the study period significant positive values of up to 200 gpm west of Norway (Fig. 6). In contrast, the area over southwestern Europe is reflected by negative geopotential anomalies of more than 50 gpm. Qualitatively similar anomaly patterns are seen in the sea-level pressure distribution (not shown). Simultaneously, the IWV (Fig. 6b) showed distinct positive anomalies of up to 9 $kg\,m^{-2}$ with a 22-day average of 24 – 28 $kg\,m^{-2}$. This finding is in line with the sequential progression of several cut-off lows approaching southwestern Europe and leading to repeating the advection of warm and moist air masses towards central and western Europe during the study period.

3.1.1 North Atlantic-European Weather Regimes

In terms of the North Atlantic-European weather regimes, the large-scale flow situation in May was dominated by simultaneously active life cycles of a Zonal regime (ZO; **dark** red in Fig. 7**a**) and European Blocking (EuBL; green). Climatologically, the Zonal regime is characterized by a negative 500 hPa geopotential height anomaly centered over southern Greenland and Iceland, accompanied by a weak positive anomaly over central Europe **(cf. Supplementary Fig. 1)**. The climatological European Blocking regime is characterized by a strong positive geopotential height anomaly over the North Sea region, and a weak negative anomaly over Baffin Bay.

The strong projection in both regimes in May suggests that both the cyclonic anomaly in the Icelandic region and the positive anticyclonic anomaly over Europe were pronounced but altered in their intensities – as discussed in the previous section. The alternating dominance of either regime in the first three weeks of May (Fig. 7**a**) reflects the change of zonal to meridional circulation and the persistent blocking situation during our study period. It is striking that enhanced convection and thunderstorm activity over Europe co-occurred with a weakening of the projection in the Zonal regime (**see Section before**). Specifically, the first period of widespread thunderstorms (9 – 16 May; cf. Fig. 2) coincides with a weakening of zonal conditions and a dominance of European Blocking from 11 to 18 May. This is interrupted by more zonal conditions from 19 to 21 May, leading to a substantial weakening of convective activity. The convectively most active period from 26 May to 1 June co-occurs with a very strong projection into European Blocking and ends when the blocking decays. On 3 June, a transition into the Atlantic Ridge regime occurs, with blocking shifting into the Northeast Atlantic and western Europe, which coincides with the last episode of an increased number of convective events from 6 to 12 June.

3.1.2 Local-scale environmental conditions

During the entire May/June period, atmospheric stability was very low over large parts of the study domain as indicated by sounding data (Fig. 7**b**). The SLI values reached negative values almost every day at 12 UTC at one sounding station at least. During the first thunderstorm episode from 9 to 16 May with several heavy rain and hail events (cf. Fig. 2), several stations already show negative SLI values at some days. During the study period, all soundings (with a few exceptions) exhibit permanently negative SLI values; most of the time the values are far below the basic/strict criterion of PIP16 (cf. Sect. 2.6). For

example, the median of the SLI during the study period was lower than –3.0 K for Stuttgart, Munich, Vienna, Trappes, and Payerne. Such low values represent very conducive conditions for thunderstorm formation (e.g., Haklander and van Delden, 2003; Manzato, 2003; Sánchez et al., 2009; Kunz, 2007; Mohr and Kunz, 2013). In the ECMWF analysis (Fig. 8a), the SLI average over the study period (12 UTC) was negative for most parts of the domain except for northern Germany, where thunderstorms occurred infrequently. Furthermore, over large parts of the study domain, the strict criterion was also reached. Due to the upcoming westerly flow at the end of the study period, instability **decreased significantly and SLI returned** to positive values less conducive for deep moist convection (Fig. 7**b**).

Due to the low-pressure gradient that prevailed during the study period (Fig. 6), horizontal wind speed in the mid-troposphere was likewise exceptionally low. During the first half of May, 500 hPa wind speed (V500) was already low in the sounding data with values rarely exceeding 15 $m\,s^{-1}$ (Fig. 7**c**), but further dropped significantly at the beginning of the study period. Averaged over the entire study period, median V500 was 7 $m\,s^{-1}$ at the Essen sounding station; at Stuttgart, Munich, and Vienna values were even lower at around 5 $m\,s^{-1}$. At the other three stations in France and Switzerland, the median was between 8 and 10 $m\,s^{-1}$. The observations are in line with ECMWF analysis, where V500 was between 5 and 10 $m\,s^{-1}$ on average (particularly low in large parts of Germany and Austria; Fig. 8b).

Due to the very low wind speed near the surface, V500 is almost similar to BWS from ECMWF analysis (12 UTC; Fig. 8c). Mean values of BWS between 5 and 10 $m\,s^{-1}$ across the study area (except of the Pyrenees region) are a strong indication that the majority of storms did not developed into highly organized convective systems such as squall lines, MCS or supercells. The following analyses are relying on V500 instead of BWS, especially because of the very unusually low wind speed at 500 hPa. It should be noted that the values for the deep layer shear (speed shear) are even lower compared to BWS (3 – 9 $m\,s^{-1}$; not shown).

3.2 Air mass origin and paths during the event

The investigation of sounding data revealed an exceptional air mass, which conserved its key properties conducive to convection in the entire study period. This finding together with the low-pressure gradient associated with the blocking anticyclone over the European sector (Fig. 6) suggests that the air mass was relatively stationary in western and central Europe during the study period. To test this hypothesis, 10-day kinematic backward trajectories are calculated to investigate the Lagrangian history and paths of moist, lower-tropospheric air masses. Though backward trajectories are started from all six sounding stations, Bordeaux, Stuttgart, and Vienna are chosen as representative locations for the following analysis.

The median trajectory pathways during the entire study period 22 May to 12 June consistently show that air masses originated west of the sounding stations and reached those in a southwesterly flow (Fig. 9a). Already ten days prior to reaching the area of the sounding stations, two thirds of the air masses were located over the Atlantic-European sector. Though about 50 % of the air masses were transported over a distance of 5,000 km (Fig. 9b), the median distance from their initial location (i.e., Bordeaux, Stuttgart, Vienna) never exceeded more than 2,000 km (Fig. 9c). This clearly indicates that air masses re-circulated while approaching the area of the sounding stations. Five days prior to arriving

at the location, trajectories were mostly located over Europe (bold ellipses) and within a radius of 1,000 km around the sounding stations.

3.3 Thunderstorms related to cut-off lows

After having shown that a quasi-stationary air mass, which was conducive to convection prevailed over vast parts of central Europe during the study period, we now explore cut-off low activity as potential trigger for thunderstorms. The blocking situation over central Europe and the North Sea during the study period was accompanied by a negative geopotential height anomaly over the Iberian Peninsula (Fig. 6), which corresponds well with a significantly enhanced frequency of PV cut-offs of more than 50 % in the Bay of Biscay region (Fig. 10). This region of enhanced PV cut-off frequencies expands over **much** of Spain, western France and some parts of the British Isles with frequencies often above 25 %, but does not reach Germany or eastern Europe. The fact that relatively high PV cut-off frequencies expand over a larger region of western Europe **(Fig. 10)** underlines that multiple individual PV cut-offs form on the upstream flank of the blocking ridge **(see Fig. 5)**, and intermittently move across Iberia, France, the British Isles, the North Sea, and Germany.

In such a configuration, filaments of positive PV that separate from the main PV cut-off may favour lifting on their downstream flank and **help to** trigger deep moist convection over larger areas. This relation is **exemplified by** a 2-day period from 31 May to 1 June representing the end of the period with the most lightning activity and ESWD reports. Here, more than 700,000 lightning strikes were measured over the study domain (black bars in Fig. 11) and more than 70 % of these can be attributed to PV cut-off activity (light grey bars). On 31 May, in the early afternoon, thunderstorms primarily affected Belgium and the Netherlands first (Fig. 12a), before lightning activity re-emerged over central and northern France, Switzerland, and various parts of Germany (Fig. 12b). Several of these events were documented by heavy rain reports in the ESWD (cf. Fig. 2). During the following night, the slow-moving multicellular system moved from Switzerland northwards affecting the southwestern and the western parts of Germany (Fig. 12c,d; cf. Sect. 3). While the system dissipated in the late morning over the border region of Germany and Belgium, severe thunderstorms developed again over eastern and northern Germany, Czech Republic, western Poland, and the Pyrenees (Spain; Fig. 12e,f). The link to upper-level PV filaments becomes apparent by carefully investigating the 6-hour evolution of the identified cut-off low masks (Fig. 12; cf. Sect. 2.5). Additionally, the area of negative ω values indicates upward vertical motion over larger areas (**light blue**). Generally, this point is expected downstream of a trough/PV cut-off due to vertically increasing advection of PV in combination with layer thickness advection and destabilization underneath the high PV air, which is well represented in our example. On 31 May, a narrow trough accompanied by the cut-off low (C3) approached from the Atlantic to Iberia (cf. Fig. 5e). The areas of ascent on 31 May (Fig. 12a) correspond well with the regions of thunderstorm development in southeastern Germany, central France and the Netherlands (Fig. 12b). From 12 UTC until 18 UTC the next day, this trough narrowed while moving gradually northeastward accompanied by enhanced lightning activity moving from Central France and southern Germany to northeastern Germany and Poland (Fig. 12e,f). It is especially apparent that the multicellular system, which developed in the evening hours of 31 May ~~and was already mentioned at the end of~~ (Section 3), emerged in a region of negative ω values ahead of the trough (Fig. 12c). On 1 June ascent occurs

further to the east over Austria, the Czech Republic and northeastern Germany (Fig. 12e), which agrees well with the location of thunderstorm initiation.

The above discussion of PV filament evolution and lightning activity from 31 May to 1 June revealed an apparent link of this feature with lighting activity confined to the downstream side of PV filaments, where lifting is favoured. Considering the entire study period, we found 54 % of the lightning linked to a nearby PV cut-off (Fig. 11). Examining individual days reveals that on the day with the highest number of lightning detections (29 May) over 85 % of these events can be linked to a PV cut-off. Six out of eight days with the highest number of lightning flashes were between 27 May to 1 June. During this period, more than 75 % of the lightning strikes can be connected with one of the PV cut-offs. We conclude that cut-off low activity provided the necessary environment that favoured lifting within the prevailing unstable air mass and thus helped to trigger widespread thunderstorm activity in western and central Europe during this period.

4 Historical context

In this section, we assess the exceptional nature of the thunderstorm event, by relating the observed **rainfall totals**, the prevailing environmental conditions, and the occurrence of cut-off systems to the long-term data record.

4.1 Return periods of rainfall and propagation speed of convective cells

To estimate the severity of the rainfalls with respect to the rainfall climatology, we computed return periods (RPs) for each day during the study period in the REGNIE long-term record based on Equation (3). Afterward, we determined the highest RP (largest 24-hour rain total) for each grid point. Because long-term (> 50 years), highly-resolved ($1\,\mathrm{km}^2$) and area-wide precipitation data are available only for Germany, we restrict our analysis to this area. **REGNIE data derived from measurements at climate stations certainly underestimate precipitation peaks, but this is the case both for the study period and the 67-years reference period.**

Extreme precipitation generally occurred locally, and only a few smaller regions were affected by high rainfall totals exceeding RPs of 5 years (Fig. 13). RPs in excess of 10 years were restricted to the southern parts of Germany (south of 52°N), except for a few grid points south of Berlin. Most of the precipitation fields with higher RPs occurred as clusters; for example, those near the border to France in Rhineland Palatinate and the Saarland (near Saarbruecken), northeast of Stuttgart, around Bad-Elster Sohl, or north of Munich. Several local maxima have RPs of up to 50 years, but a few hot spots, unevenly distributed in southern Germany, reach values in excess of 200 years (e.g., the observation in Bad Elster-Sohl; cf. Sect. 3). For those locations, of course, precipitation was extreme, partly with new all-year records. Several hot spots have an almost circular shape with the highest value located in the center. **This is not an artefact of insufficient gauge density (i.e. only one station is considered), since most fields take several precipitation stations into account (not shown).**

This characteristic likely reflects the very slow propagation of the thunderstorms, which was substantially lower during the study period compared to climatology (Fig. 4). Generally, convective storms detected between 2005 and 2017 (May/June: 3,428 cells) show significantly higher values of $10.2 \pm 4.9\,\mathrm{m\,s^{-1}}$ (mean $\pm$ std) and $9.5\,\mathrm{m\,s^{-1}}$ (median) compared to $5.9 \pm 2.9\,\mathrm{m\,s^{-1}}$

and 5.2 m s^{-1} in the study period. Only 14.4 % of all detected cells show values below 5 m s^{-1}, which differs significantly from the proportion in the study period with 47.3%. 15.5 % of the events propagated with a speed of at least 15 m s^{-1} (study period only 1.5%; cf. Sect. 3.1.2).

4.2 Environmental conditions

We begin the analysis of the environmental conditions by comparing the SLI and V500 values observed at the seven sounding stations during the study period with **comparably low values during a 30-year period. The latter is represented by the annual minimum of 22-day (same duration as study period) running mean values for May and June during 1981 and 2010. The box-and-whisker plots (Fig. 14) on the left represent conditions during our study period (all 22 daily values) and on the right the historical situation (in sum 30 values)**. Recall that the low values for both SLI and V500 were the peculiarity during the 2018 thunderstorm episode. By doing so, each of the 30 values taken into account in the right box-plot of each station has the same temporal dimension (running mean of a 22-day period) as the median in the left box-plot of each station.

Both for atmospheric stability and mid-tropospheric flow speed, the interquartile range (the middle 50 % of all values) of the left box-plot is mostly lower than the interquartile range of the right box-plot, illustrating the exceptional environmental conditions of the 2018 thunderstorm episode. This applies in particular to the stations in Germany and Austria; stations in France and in Switzerland tend to overlap (slightly) between the two interquartile ranges. As already mentioned in Sect. 3.1.2, a large portion of SLI and V500 values during the event (left box-plot) are well below the basic and strict thresholds (cf. Sect. 2.6).

To elaborate on both the peculiarity of the co-occurrence of low stability and weak mid-tropospheric flow and the persistence, we investigate the probability of concurrent events (CE) by following the methodology of PIP16 (see Sect. 2.6) using the same basic criterion. The **event persistences** of CE for each of the seven sounding stations during the extended study period in 2018 varies between 5 (Trappes) and 28 days (Munich; cf. legend in Fig. 15). At all three German stations, the defined concurrent conditions prevailed over an extraordinarily long period (Essen: 17 days incl. 3 skip days; Stuttgart: 21 days incl. 1 skip days; Munich 28 days incl. 3 skip days).

In order to assess the occurrence probability of **event persistences of CE with long duration, we compare the event persistences for the 2018 thunderstorm episode with a frequency analysis of CE between 1981 and 2017 (May/June; Fig. 15). In doing so, the different amount of a certain event persistence with the length n from the past between 1981 and 2017 are determined for each sounding station. Subsequently, the relative frequency of the event persistence n per station in Figure 15 is determined by dividing the absolute number of event persistence by the total number of all events. For example, the total number of all events** is approximately 100 for Trappes, Bordeaux, and Essen, approximately 150 for Stuttgart and Payerne, and approximately 200 for Munich and Vienna reflecting the climatological distribution (north-to-south and west-to-east gradient) of atmospheric stability (Mohr and Kunz, 2013).

The exceptional nature of the atmospheric conditions in 2018 is supported by the fact that, for example, the maximum **event persistence** of 19 days between 1981 and 2017 (observed in Vienna) was exceeded in 2018 by two of the considered

sounding stations (Stuttgart, Munich). Additionally, when examining the individual stations, it can be seen that the CE **event persistences** of 2018 at the stations Stuttgart, Essen, Munich and Payerne have never been observed since 1981. The same applies to the Stuttgart sounding compared with the results in PIP16, where so far a maximum CE **event persistence** of 16 days (1960 – 2014, but summer half-year) has been calculated. Furthermore, the relative frequency of CE at the other stations (Trappes, Bordeaux, Vienna) is also rare (0.5 – 2 %).

4.3 Cut-off lows

In May and June, cut-off lows particularly affected southern Europe and the Mediterranean region. The highest frequency during the climatological period from 1981 to 2010 is found over Portugal and Turkey but with values **of around 4 %** (contour in Fig. 16; cf. Nieto et al., 2007b; Wernli and Sprenger, 2007). **This means that during a 22-day period (same time horizon of the study period) in May and June an average of 0.9 days (4 % of 22 days) with PV cut-off can be expected.** During the 2018 thunderstorm episode, the anomaly of the PV cut-off frequency from the climatological mean was exceptionally large with maximum values of around 40 % confined to northern Iberia and the Bay of Biscay in western Europe. **This means that in 2018 a PV cut-off was additionally up to 10 times higher than the climatological mean, resulting in 9 additional days.** The region of anomalous PV cut-off activity expands northward over the British Isles and the adjacent Atlantic Ocean and the North Sea, still with an excess of 20 % (**additional 4 days compared to climatological mean**). In other regions, PV cut-off occurrence was similar to the climatological mean. **As an orientation, note that the standard deviation of the cut-off low frequency between 1981 to 2010 (May/June) is 3 % over northern Iberia and the Bay of Biscay and between 1 and 2 % over the British Isles (not shown).** We conclude that the unusual blocking situation over Europe effectively caused cut-off formation on its upstream flank, which then supported a (synoptic) lifting mechanism – the third ingredient for thunderstorm development, together with instability and available moisture.

5 Discussion

~~It is well known that deep moist convection depends on three necessary but not sufficient ingredients (e.g., Johns and Doswell, 1992; Fuelberg and Biggar, 1994; Trapp, 2013): any kind of instability (conditional, latent, potential) over a layer of sufficient depth, sufficient moisture in the lower troposphere, and a lifting mechanism for the triggering of convection. A further relevant condition for the evolution of deep moist convection is the vertical wind shear or, more generally, the wind at mid-tropospheric levels, which is decisive not only for the organizational form, the longevity and thus the severity of the convective storms (e.g., Weisman and Klemp, 1982; Thompson et al., 2007; Dennis and Kumjian, 2017), but also for their propagation (Corfidi, 2003).~~

In this study, we investigated the synoptic characteristics of an unusual three-week period of thunderstorm activity in central Europe in May/June 2018. Interestingly, atmospheric blocking was key to providing the large-scale setting conducive for convective in its vicinity. Because of the influence of large-scale mechanisms related to the block and affecting the entire continent, a very high number of thunderstorms affected large parts of western and central Europe during an unusually long period of three weeks. At the beginning of the thunderstorm period, southwesterly flow induced the advection of warm and

moist air masses into central Europe. Several studies have identified such a flow to provide convection-favouring conditions (e.g., van Delden, 2001; Kapsch et al., 2012; Mohr, 2013; Merino et al., 2014; Wapler and James, 2015; Nisi et al., 2016; Piper et al., 2019; Mohr et al., 2019). Subsequently, the low-pressure gradient associated with the blocking anticyclone over the (adjacent) European sector prevented a significant air mass change. Thus, moist and conditionally unstable stratified air masses were trapped in a stationary flow on the southern flank of high pressure for more than three weeks **(and were re-circulated)**. A few authors have already identified atmospheric blocking as a relevant influencer for widespread thunderstorms. PIP16, for example, showed that the exceptional thunderstorm episode in 2016 in Germany was related to the sequence of Scandinavian and European Blocking. Santos and Belo-Pereira (2019) identified a blocking-like dynamical structure in addition to a Western European and a Scandinavian trough to be responsible for approximately three-quarters of all hail events across Portugal. By combining ERA-Interim reanalysis and lightning detections over a 14-years period, Mohr et al. (2019) found that the presence of a block over the Baltic Sea is frequently associated with increased odds of thunderstorm occurrence due to convection-favouring conditions on its western flank (southwesterly advection of warm, moist and unstable air masses).

Upper-level cut-off lows or filaments of high PV that separate from the main PV cut-off were key in creating conditions conducive for convective activity on the meso-scale. Associated lifting can increase CAPE and reduce Convective inhibition (CIN) or can generate instability, if an entire column is lifted bodily until complete saturation in case of potential instability (Markowski and Richardson, 2010). On several days during the peak thunderstorm activity, we found that the majority of thunderstorms (based on lightning detections) can be related to a PV cut-off that favours lifting on its downstream flank. The large positive anomaly in PV cut-off frequency, which seems to be relevant for the exceptionally high number of thunderstorms during the study period, in turn was also related to atmospheric blocking. The latter repeatedly lead to the elongation of troughs on its upstream flanks, which finally led to several cut-off lows. The general flow patterns consisting of this spatially extended ridge flanked by troughs persisted over a period of three weeks.

Heavy rain events are a result of continuously high rain rates, whereby the duration of an event is linked to its propagation speed and the size of the convective system (Doswell et al., 1996). In addition, a high concentration of water vapour at low levels in the presence of strong updrafts, high environmental relative humidity, significant cloud depth below the freezing level contribute to maximize rain accumulations, and potentially weak vertical wind shear, which tend to be correlated with weak mid-tropospheric winds (Markowski and Richardson, 2010, Chap. 10.4). Due to the low propagation speeds, which contributes to long rainfall duration during the thunderstorm episode in 2018, and high rain rates (60 mm h^{-1} continuously over 50 min), some of the thunderstorms were able to produce torrential amounts of rain. Furthermore, the stagnant flow at mid-tropospheric levels and thus the low vertical wind shear as a consequence of the blocking (cf. PIP16; Mohr et al., 2019) were also conducive and frequently prevented most thunderstorms from developing into organized systems such as large MCS or supercells (cf. Weisman and Klemp, 1982; Doswell and Evans, 2003; Markowski and Richardson, 2010). Most of the thunderstorms formed as short-lived isolated cells or slow-moving multicellular clusters.

6 Summary and Conclusions

In our study, we investigated an exceptionally large number of thunderstorms in western and central Europe over a three-week period, mid-May to mid-June 2018, using a combination of observational data and model data to gain a more holistic view of the prevailing dynamical and thermodynamical conditions and the decisive trigger mechanisms for this unusual thunderstorm episode. Additional data over a climatological period helped to place the event in its historical context. The 2018 thunderstorm episode was exceptional due to several reasons: (i) the unusual large number of several thousand thunderstorms that caused more than 5 million lightning strikes (all types) in the study area; (ii) the combination of low stability (negative Lifted Index) and low wind speed at mid-tropospheric levels ($\leqslant 5\,\mathrm{m\,s^{-1}}$ at some locations) that prevailed almost every day during the 22-day period; (iii) the large cut-off low frequency that was responsible for the majority of convection triggering; and (iv) the high rainfall totals with several new records (e.g., Dietenhofen 86 mm / 1 h) mainly as a consequence of the low propagation speed of the storms **in combination with high rain rates** leading to several pluvial flash floods.

The other main conclusions drawn from our analyses are:

- Atmospheric blocking, albeit frequently associated with heatwaves and droughts, provided large-scale environmental conditions favouring convection in its vicinity when unstably stratified air masses are advected **into Europe** and/or become entrapped in stagnant flow.

- In the present paper, blocking is accompanied by a high cut-off frequency on its upstream side, which together with filaments of high PV **provided the meso-scale setting** for deep moist convection. Compared to climatology, the number of cut-off lows in parts of the study area during the study period was up to 10 times higher.

- The exceptional persistence of low stability combined with weak wind speed in the mid-troposphere prevailing over more than three weeks in some regions, especially in Germany and Austria, has never been observed during the past climatological period of 30 years. This situation was similar to the 2016 thunderstorm episode documented by PIP16, but with a much longer persistence.

- Blocking often associated with low mid-tropospheric wind speeds/low wind shear (cf. Mohr et al., 2019) reduces the development in severe organized convective systems. However, because of the low propagation speed of the storms related to the low-pressure gradient within the block, torrential rainfalls can occur on a local scale.

A growing understanding of the relationship between atmospheric blocking and deep moist convection can enhance – due to the associated persistence – the forecast horizon of thunderstorms on sub-seasonal time scales beyond the classical weather forecast time scale of a few days. This may, for example, help with disaster management, large outdoor activities, and the agriculture sector. It is only helpful, however, if blocked areas are correctly predicted. Recent studies show that this remains a challenge for present ~~(global/regional)~~ numerical weather prediction and climate models (Ferranti et al., 2015; Grams et al., 2018), which, for example, underestimate the blocking frequency in the Atlantic-European sector (Quinting and Vitart, 2019; Attinger et al., 2019).

In future, we intend to investigate statistically some of this study's results, such as the relationship between blocking, cut-off lows, **air mass transport,** and thunderstorm probability. Furthermore, we want to distinguish between different hazard types (hail, heavy rain, gusts) and associated types of thunderstorms and blocking regimes that reveal possible differences in atmospheric processes (e.g., jet stream).

Acknowledgements. The authors thank the various national weather service (DWD; MeteoSwiss; Météo-France; Royal Netherlands Meteorological Institute, KNMI; Zentralanstalt für Meteorologie und Geodynamik; ZAMG), the European Climate Assessment and Dataset (ECA&D) project, the Blitz-Informationsdienst von Siemens (BLIDS; namely Stephan Thern), the Integrated Global Radiosonde Archive (IGRA) and the European Severe Storms Laboratory (ESSL) for providing different observational data sets. In addition, we thank the European Centre for Medium-Range Weather Forecasts (ECMWF) for providing the operational analysis and the ERA-Interim reanalysis data. Furthermore, we thank Michael Sprenger (ETH Zurich) for compiling the ERA-Interim PV cutoff climatology and Florian Ehmele (KIT) for the post-processing of the REGINE data (return periods). The contributions of CMG, **JFQ,** and JaWa were funded by the Helmholtz Association as part of the Young Investigator Group „Sub-Seasonal Predictability: Understanding the Role of Diabatic Outflow" (SPREADOUT; grant VH-NG-1243). **We acknowledge the constructive comments two anonymous reviewers, which helped to improve the quality of the paper.**

Data availability. REGNIE (doi:10.1127/0941-2948/2013/0436), German precipitation data, and 3D radar data used in this paper are freely available for research and can be requested at DWD. Tracks of severe convective storms were calculated from the DWD radar data and are not freely available, but can be made available on request to Michael Kunz for research. Data from ECA&D can be downloaded via the project website (https://www.ecad.eu), from Météo-France via https://donneespubliques.meteofrance.fr/?fond=rubrique&id_rubrique=26, from MeteoSwiss via https://www.meteoswiss.admin.ch/home/services-and-publications/beratung-und-service/datenportal-fuer-lehre-und-forschung.html, and from ZMAG via https://www.zamg.ac.at/cms/de/klima/produkte-und-services/daten-und-statistiken/messdaten. Sounding data are available from the Integrated Global Radiosonde Archive (https://www.ncdc.noaa.gov/data-access/weather-balloon/integrated-global-radiosonde-archive) and data from the ESWD can be obtained via https://www.eswd.eu (see terms and conditions for academic or commercial use). Lightning data are not freely available, but can be requested from the Blitz-Informationsdienst von Siemens (http://blids.de). ECMWF ERA-Interim reanalysis and operational analysis are also online available via https://apps.ecmwf.int/datasets/data/interim-full-daily and the TIGGE webpage (control forecast step 0; https://apps.ecmwf.int/datasets/data/tigge). The methods to detect cut-off lows based on these data are given in Wernli and Sprenger (2007) and Sprenger et al. (2017) and for weather regimes in Grams et al. (2017).

Author contributions. All KIT authors jointly conceived the research questions of the study, continuously discussed the results and wrote the text passages for their respective contribution. SM analysed the ESWD data and together with JaWi the environmental conditions during the thunderstorm episode and in a historical context. In addition, SM wrote the introduction part together with CMG and the discussion/summary part of the paper together with MK and prepared the final draft version of the paper. JaWi also described the synoptic overview and the rainfall statistics in 2018, which were produced by HJP. The return periods of rainfall were investigated by MK, who also examined the lightning

data. **Based on LAGRANTO, JQ performed backward trajectory analysis.** MS contributed with the analyses of the storm track data (propagation speed of convective cells). RP generated the PV cut-off data and its relationship to lightning activity was analysed by JaWa and CMG. In addition, CMG contributed with the analysis of the weather regimes. Finally, all co-authors edited the final draft and provided substantial comments and constructive suggestions for scientific clarification and further improvements.

Competing interests. The authors declare that they have no conflict of interest.

Supplement. The supplement related to this article is available online at: https://doi.org/10.5194/jn-0-1-2020-supplement.

Video supplement. **Video supplement related to this paper is available from the Repository KITopen at: https://doi.org/10.5445/IR/1000118571 and https://doi.org/10.5445/IR/1000118574**.

References

Attinger, R., Keller, J. H., Köhler, M., Riboldi, J., and Grams, C. M.: Representation of atmospheric blocking in the new global non-hydrostatic weather prediction model ICON, Meteorol. Z., 28, 429–446, https://doi.org/10.1127/metz/2019/0967, 2019.

Barriopedro, D., García-Herrera, R., Lupo, A. R., and Hernández, E.: A climatology of Northern Hemisphere blocking, J. Climate, 19, 1042–1063, https://doi.org/10.1175/JCLI3678.1, 2006.

Barthlott, C., Schipper, J. W., Kalthoff, N., Adler, B., Kottmeier, C., Blyth, A., and Mobbs, S.: Model representation of boundary-layer convergence triggering deep convection over complex terrain: A case study from COPS, Atmos. Res., 95, 172–185, https://doi.org/10.1016/j.atmosres.2009.09.010, 2010.

Bennett, L. J., Browning, K. A., Blyth, A. M., Parker, D. J., and Clark, P. A.: A review of the initiation of precipitating convection in the United Kingdom, Q. J. R. Meteorol. Soc., 132, 1001–1020, https://doi.org/10.1256/qj.05.54, 2006.

Bieli, M., Pfahl, S., and Wernli, H.: A Lagrangian investigation of hot and cold temperature extremes in Europe, Q. J. R. Meteorol. Soc., 141, 98–108, https://doi.org/10.1002/qj.2339, 2015.

Bronstert, A., Agarwal, A., Boessenkool, B., Crisologo, I., Fischer, M., Heistermann, M., Köhn-Reich, L., López-Tarazón, J. A., Moran, T., Ozturk, U., Reinhardt-Imjela, C., and Wendi, D.: Forensic hydro-meteorological analysis of an extreme flash flood: The 2016-05-29 event in Braunsbach, SW Germany, Sci. Total Environ., 630, 977–991, https://doi.org/10.1016/j.scitotenv.2018.02.241, 2018.

Browning, K., Blyth, A., Clark, P., Corsmeier, U., Morcrette, C., Agnew, J., Bamber, D., Barthlott, C., Bennett, L., Beswick, K., Bitter, M., Bozier, K., Brooks, B., Collier, C., Cook, C., Davies, F., Deny, B., Feuerle, T., Forbes, R., Gaffard, C., Gray, M., Rolf Hankers, R., Hewison, T., Kalthoff, N., Khodayar, S., Kohler, M., Kottmeier, C., Kraut, S., Kunz, M., Ladd, D., Lenfant, J., Marsham, J., McGregor, J., Nicol, J., Norton, E., Parker, D., Perry, F., Ramatschi, M., Ricketts, H., Roberts, N., Russell, A., Schulz, H., Slack, E., Vaughan, G., Waight, J., Watson, R., Webb, A., and Wieser, A.: The Convective Storms Initiation Project, Bull. Am. Meteorol. Soc., 88, 1939–1955, https://doi.org/10.1175/BAMS-88-12-1939, 2007.

Corfidi, S. F.: Cold pools and MCS propagation: Forecasting the motion of downwind-developing MCSs, Weather Forecast., 18, 997–1017, https://doi.org/10.1175/1520-0434(2003)018<0997:CPAMPF>2.0.CO;2, 2003.

Dee, D. P., Uppala, S. M., Simmons, A. J., Berrisford, P., Poli, P., Kobayashi, S., Andrae, U., Balmaseda, M. A., Balsamo, G., Bauer, P., Bechtold, P., Beljaars, A. C. M., Van De Berg, L., Bidlot, J., Bormann, N., Delsol, C., Dragani, R., Fuentes, M., Geer, A. J., Haimberger, L., Healy, S. B., Hersbach, H., Hólm, E. V., Isaksen, L., Kållberg, P., Köhler, M., Matricardi, M., Mcnally, A. P., Monge-Sanz, B. M., Morcrette, J. J., Park, B. K., Peubey, C., De Rosnay, P., Tavolato, C., Thépaut, J. N., and Vitartv, F.: The ERA-Interim reanalysis: Configuration and performance of the data assimilation system, Q. J. R. Meteorol. Soc., 137, 553–597, https://doi.org/10.1002/qj.828, 2011.

Dennis, E. J. and Kumjian, M. R.: The impact of vertical wind shear on hail growth in simulated supercells, J. Atmos. Sci., 74, 641–663, https://doi.org/10.1175/JAS-D-16-0066.1, 2017.

Dole, R. M. and Gordon, N. D.: Persistent anomalies of the extratropical Northern Hemisphere wintertime circulation: Geographical distribution and regional persistence characteristics, Mon. Weather Rev., 111, 1567–1586, https://doi.org/10.1175/1520-0493(1983)111<1567:PAOTEN>2.0.CO;2, 1983.

Doswell, C. A. and Evans, J. S.: Proximity sounding analysis for derechos and supercells: An assessment of similarities and differences, Atmos. Res., 67, 117–133, https://doi.org/10.1016/S0169-8095(03)00047-4, 2003.

Doswell, C. A., Brooks, H. E., and Maddox, R. A.: Flash flood forecasting: An ingredients-based methodology, Weather Forecast., 11, 560–581, https://doi.org/10.1175/1520-0434(1996)011<0560:FFFAIB>2.0.CO;2, 1996.

Dotzek, N., Groenemeijer, P., Feuerstein, B., and Holzer, A. M.: Overview of ESSL's severe convective storms research using the European Severe Weather Database ESWD, Atmos. Res., 93, 575–586, https://doi.org/10.1016/j.atmosres.2008.10.020, 2009.

Drüe, C., Hauf, T., Finke, U., Keyn, S., and Kreyer, O.: Comparison of a SAFIR lightning detection network in northern Germany to the operational BLIDS network, J. Geophys. Res. Atmos., 112, D18 114, https://doi.org/10.1029/2006JD007680, 2007.

Durre, I., Vose, R. S., and Wuertz, D. B.: Overview of the integrated global radiosonde archive, J. Climate, 1151, 53–68, https://doi.org/10.1175/JCLI3594.1, 2006.

DWD: Schadensrückblick des Deutschen Wetterdienstes: Gefährliche Wetterereignisse und Wetterschäden in Deutschland 2018, Deutscher Wetterdienst (DWD), Offenbach, Germany. Available from: https://www.dwd.de/DE/presse/pressemitteilungen/DE/2018/20181213_schadensrueckblick2018_news.html (Accessed 6 March 2020), 2018a.

DWD: REGNIE: Regionalisierte Niederschläge Verfahrensbeschreibung und Nutzeranleitung, Deutscher Wetterdienst (DWD), Abteilung Hydrometeorologie, Offenbach, Germany. Available from: https://www.dwd.de/DE/leistungen/regnie/regnie.html?nn=353366 (Accessed 13 December 2019), 2018b.

DWD: RADOLAN/RADVOR: Hoch aufgelöste Niederschlagsanalyse und -vorhersage auf der Basis quantitativer Radar-und Ombrometerdaten für grenzüberschreitende Fluss-Einzugsgebiete von Deutschland im Echtzeitbetrieb – Beschreibung des Kompositformats Version 2.5, Tech. rep., Deutscher Wetterdienst (DWD): Abteilung Hydrometeorologie, Offenbach, Germany. Available from: https://www.dwd.de/DE/leistungen/radolan/radolan.html (Accessed 6 March 2020), 2019.

Ehmele, F. and Kunz, M.: Flood-related extreme precipitation in Southwestern Germany: Development of a two-dimensional stochastic precipitation model, Hydrol. Earth Syst. Sci., 23, 1083–1102, https://doi.org/10.5194/hess-23-1083-2019, 2019.

Enno, S.-E., Sugier, J., Alber, R., and Seltzer, M.: Lightning flash density in Europe based on 10 years of ATDnet data, Atmos. Res., 235, 104 769, https://doi.org/10.1016/j.atmosres.2019.104769, 2020.

ESSL: ESWD Event reporting criteria, Last revision: May 10, 2014, European Severe Storms Laboratory e.V., Munich, Germany. Available from: https://www.eswd.eu/docs/ESWD_criteria_en.pdf (Accessed 13 December 2019), 2014.

Ferranti, L., Corti, S., and Janousek, M.: Flow-dependent verification of the ECMWF ensemble over the Euro-Atlantic sector, Q. J. R. Meteorol. Soc., 141, 916–924, https://doi.org/10.1002/qj.2411, 2015.

Galway, J. G.: The lifted index as a predictor of latent instability, Bull. Am. Meteorol. Soc., 37, 528–529, https://doi.org/10.1175/1520-0477-37.10.528, 1956.

Grams, C. M. and Blumer, S. R.: European high-impact weather caused by the downstream response to the extratropical transition of North Atlantic Hurricane Katia (2011), Geophys. Res. Lett., 42, 8738–8748, https://doi.org/10.1002/2015GL066253, 2015.

Grams, C. M., Binder, H., Pfahl, S., Piaget, N., and Wernli, H.: Atmospheric processes triggering the central European floods in June 2013, Nat. Hazards Earth Syst. Sci., 14, 1691–1702, https://doi.org/10.5194/nhess-14-1691-2014, 2014.

Grams, C. M., Beerli, R., Pfenninger, S., Staffell, I., and Wernli, H.: Balancing Europe's wind-power output through spatial deployment informed by weather regimes, Nat. Clim. Change, 7, 557–562, https://doi.org/10.1038/nclimate3338, 2017.

Grams, C. M., Magnusson, L., and Madonna, E.: An atmospheric dynamics perspective on the amplification and propagation of forecast error in numerical weather prediction models: A case study, Q. J. R. Meteorol. Soc., 144, 2577–2591, https://doi.org/10.1002/qj.3353, 2018.

Groenemeijer, P., Púčik, T., Holzer, A. M., Antonescu, B., Riemann-Campe, K., Schultz, D. M., Kühne, T., Feuerstein, B., Brooks, H. E., Doswell, C. A., Koppert, H.-J., and Sausen, R.: Severe convective storms in Europe: Ten years of research at the European Severe Storms Laboratory, Bull. Am. Meteorol. Soc., 98, 2641–2651, https://doi.org/10.1175/BAMS-D-16-0067.1, 2017.

Gumbel, E. J.: Statistics of Extremes, Columbia University Press, New York, USA, 1958.

Haklander, A. J. and van Delden, A.: Thunderstorm predictors and their forecast skill for the Netherlands, Atmos. Res., 67–68, 273–299, https://doi.org/10.1016/S0169-8095(03)00056-5, 2003.

Handwerker, J.: Cell tracking with TRACE3D — A new algorithm, Atmos. Res., 61, 15–34, https://doi.org/10.1016/S0169-8095(01)00100-4, 2002.

Hoskins, B. J., McIntyre, M. E., and Robertson, A. W.: On the use and significance of isentropic potential vorticity maps, Q. J. R. Meteorol. Soc., 111, 877–946, https://doi.org/10.1002/qj.49711147002, 1985.

Houston, A. L. and Wilhelmson, R. B.: The impact of airmass boundaries on the propagation of deep convection: A modeling-based study in a high-CAPE, low-shear environment, Mon. Weather Rev., 140, 167–183, https://doi.org/doi:10.1175/MWR-D-10-05033.1, 2012.

Huntrieser, H., Schiesser, H. H., Schmid, W., and Waldvogl, A.: Comparison of traditional and newly developed thunderstorm indices for Switzerland, Weather Forecast., 12, 108–125, https://doi.org/10.1175/1520-0434(1997)012<0108:COTAND>2.0.CO;2, 1997.

Johns, R. H. and Doswell, C. A.: Severe local storms forecasting, Weather Forecast., 7, 588–612, https://doi.org/10.1175/1520-0434(1992)007<0588:SLSF>2.0.CO;2, 1992.

Kapsch, M. L., Kunz, M., Vitolo, R., and Economou, T.: Long-term trends of hail-related weather types in an ensemble of regional climate models using a Bayesian approach, J. Geophys. Res., 117, D15 107, https://doi.org/10.1029/2011JD017185, 2012.

Klein Tank, A. M. G., Wijngaard, J. B., Können, G. P., Böhm, R., Demarée, G., Gocheva, A., Mileta, M., Pashiardis, S., Hejkrlik, L., Kern-Hansen, C., Heino, R., Bessemoulin, P., Müller-Westermeier, G., Tzanakou, M., Szalai, S., Pálsdóttir, T., Fitzgerald, D., Rubin, S., Capaldo, M., Maugeri, M., Leitass, A., Bukantis, A., Aberfeld, R., van Engelen, A. F. V., Forland, E., Mietus, M., Coelho, F., Mares, C., Razuvaev, V., Nieplova, E., Cegnar, T., Antonio López, J. A., Dahlström, B., Moberg, A., Kirchhofer, W., Ceylan, A., Pachaliuk, O., Alexander, L. V., and Petrovic, P.: Daily dataset of 20th-century surface air temperature and precipitation series for the European climate assessment, Int. J. Climatol., 22, 1441–1453, https://doi.org/10.1002/joc.773, 2002.

Kunz, M.: The skill of convective parameters and indices to predict isolated and severe thunderstorms, Nat. Hazards Earth Syst. Sci., 7, 327–342, https://doi.org/10.5194/nhess-7-327-2007, 2007.

Kunz, M., Wandel, J., Fluck, E., Baumstark, S., Mohr, S., and Schemm, S.: Ambient conditions prevailing during hail events in central Europe, Nat. Hazards Earth Syst. Sci. Discuss., in review, https://doi.org/10.5194/nhess-2019-412, 2020.

Lenggenhager, S. and Martius, O.: Atmospheric blocks modulate the odds of heavy precipitation events in Europe, Clim. Dynam., 53, 4155–4171, https://doi.org/10.1007/s00382-019-04779-0, 2019.

Lenggenhager, S., Croci-Maspoli, M., Brönnimann, S., and Martius, O.: On the dynamical coupling between atmospheric blocks and heavy precipitation events: A discussion of the southern Alpine flood in October 2000, Q. J. R. Meteorol. Soc., 145, 530–545, https://doi.org/10.1002/qj.3449, 2018.

Manzato, A.: A climatology of instability indices derived from Friuli Venezia Giulia soundings, using three different methods, Atmos. Res., 67, 417–454, https://doi.org/10.1016/S0169-8095(03)00058-9, 2003.

Markowski, P. and Richardson, Y.: Mesoscale meteorology in midlatitudes, John Wiley & Sons, Chichester, UK, 2010.

Martius, O., Sodemann, H., Joos, H., Pfahl, S., Winschall, A., Croci-Maspoli, M., Graf, M., Madonna, E., Mueller, B., Schemm, S., Sedlacek, J., Sprenger, M., and Wernli, H.: The role of upper-level dynamics and surface processes for the Pakistan flood of July 2010, Q. J. R. Meteorol. Soc., 139, 1780–1797, https://doi.org/10.1002/qj.2082, 2013.

Merino, A., Wu, X., Gascón, E., Berthet, C., García-Ortega, E., and Dessens, J.: Hailstorms in southwestern France: Incidence and atmospheric characterization, Atmos. Res., 140–141, 61–75, https://doi.org/10.1016/j.atmosres.2014.01.015, 2014.

Michel, C. and Rivière, G.: The link between Rossby wave breakings and weather regime transitions, J. Atmos. Sci., 68, 1730–1748, https://doi.org/10.1175/2011JAS3635.1, 2011.

Michelangeli, P.-A., Vautard, R., and Legras, B.: Weather regimes: Recurrence and quasi stationarity, J. Atmos. Sci., 52, 1237–1256, https://doi.org/10.1175/1520-0469(1995)052<1237:WRRAQS>2.0.CO;2, 1995.

Mohr, S.: Änderung des Gewitter- und Hagelpotentials im Klimawandel, Ph.D. thesis, Wiss. Berichte d. Instituts für Meteorologie und Klimaforschung des Karlsruher Instituts für Technologie, Vol. 58, KIT Scientific Publishing, Karlsruhe, Germany, https://doi.org/10.5445/KSP/1000033828, 2013.

Mohr, S. and Kunz, M.: Recent trends and variabilities of convective parameters relevant for hail events in Germany and Europe, Atmos. Res., 123, 211–228, https://doi.org/10.1016/j.atmosres.2012.05.016, 2013.

Mohr, S., Wandel, J., Lenggenhager, S., and Martius, O.: Relationship between atmospheric blocking and warm season thunderstorms over western and central Europe, Q. J. R. Meteorol. Soc., 145, 3040–3056, https://doi.org/10.1002/qj.3603, 2019.

Morcrette, C., Lean, H., Browning, K., Nicol, J., Roberts, N., Clark, P., Russell, A., and Blyth, A.: Combination of mesoscale and synoptic mechanisms for triggering an isolated thunderstorm: Observational case study of CSIP IOP 1, Mon. Weather Rev., 135, 3728–3749, https://doi.org/10.1175/2007MWR2067.1, 2007.

Munich Re: Natural catastrophe statistics online – the new NatCatSERVICE analysis tool, Munich Re, Munich, Germany. Available from: https://www.munichre.com/en/reinsurance/business/non-life/natcatservice/index.html (Accessed 13 December 2019), 2019.

Nachtnebel, H.-P.: New strategies for flood risk management after the catastrophic flood in 2002 in Europe, in: Third DPRI-IIASA International Symposium on Integrated Disaster Risk Management: Coping with Regional Vulnerability, Full Conference Proceedings; 3-5 July 2003, Kyoto International Conference Hall, Kyoto, Japan, 2003.

Nieto, R., Gimeno, L., Añel, J. A., De la Torre, L., Gallego, D., Barriopedro, D., Gallego, M., Gordillo, A., Redaño, A., and Delgado, G.: Analysis of the precipitation and cloudiness associated with COLs occurrence in the Iberian Peninsula, Meteorol. Atmos. Phys., 96, 103–119, https://doi.org/10.1007/s00703-006-0223-6, 2007a.

Nieto, R., Gimeno, L., De la Torre, L., Ribera, P., Barriopedro, D., García-Herrera, R., Serrano, A., Gordillo, A., Redano, A., and Lorente, J.: Interannual variability of cut-off low systems over the European sector: The role of blocking and the Northern Hemisphere circulation modes, Meteorol. Atmos. Phys., 96, 85–101, https://doi.org/10.1007/s00703-006-0222-7, 2007b.

Nieto, R., Sprenger, M., Wernli, H., Trigo, R. M., and Gimeno, L.: Identification and climatology of cut-off lows near the tropopause, Ann. NY Acad. Sci., 1146, 256–290, https://doi.org/10.1196/annals.1446.016, 2008.

Nisi, L., Martius, O., Hering, A., Kunz, M., and Germann, U.: Spatial and temporal distribution of hailstorms in the Alpine region: A long-term, high resolution, radar-based analysis, Q. J. R. Meteorol. Soc., 142, 1590–1604, https://doi.org/10.1002/qj.2771, 2016.

Ozturk, U., Wendi, D., Crisologo, I., Riemer, A., Agarwal, A., Vogel, K., López-Tarazón, J. A., and Korup, O.: Rare flash floods and debris flows in southern Germany, Sci. Total Environ., 626, 941–952, https://doi.org/10.1016/j.scitotenv.2018.01.172, 2018.

Pfahl, S. and Wernli, H.: Quantifying the relevance of atmospheric blocking for co-located temperature extremes in the Northern Hemisphere on (sub-)daily time scales, Geophys. Res. Lett., 39, L12 807, https://doi.org/10.1029/2012GL052261, 2012a.

Pfahl, S. and Wernli, H.: Quantifying the relevance of cyclones for precipitation extremes, J. Climate, 25, 6770–6780, https://doi.org/10.1175/JCLI-D-11-00705.1, 2012b.

Piaget, N., Froidevaux, P., Giannakaki, P., Gierth, F., Martius, O., Riemer, M., Wolf, G., and Grams, C. M.: Dynamics of a local Alpine flooding event in October 2011: Moisture source and large-scale circulation, Q. J. R. Meteorol. Soc., 141, 1922–1937, https://doi.org/10.1002/qj.2496, 2015.

Piper, D. and Kunz, M.: Spatiotemporal variability of lightning activity in Europe and the relation to the North Atlantic Oscillation teleconnection pattern, Nat. Hazards Earth Syst. Sci., 17, 1319–1336, https://doi.org/10.5194/nhess-17-1319-2017, 2017.

Piper, D., Kunz, M., Ehmele, F., Mohr, S., Mühr, B., Kron, A., and Daniell, J.: Exceptional sequence of severe thunderstorms and related flash floods in May and June 2016 in Germany. Part I: Meteorological background, Nat. Hazards Earth Syst. Sci., 16, 2835–2850, https://doi.org/10.5194/nhess-16-2835-2016, 2016.

Piper, D. A., Kunz, M., Allen, J. T., and Mohr, S.: Investigation of the temporal variability of thunderstorms in Central and Western Europe and the relation to large-scale flow and teleconnection patterns, Q. J. R. Meteorol. Soc., 145, 3644–3666, https://doi.org/10.1002/qj.3647, 2019.

Poelman, D. R., Schulz, W., Diendorfer, G., and Bernardi, M.: The European lightning location system EUCLID – Part 2: Observations, Nat. Hazards Earth Syst. Sci., 16, 607–616, https://doi.org/10.5194/nhess-16-607-2016, 2016., 2016.

Portmann, R., Crezee, B., Quinting, J., and Wernli, H.: The complex life cycles of two long-lived potential vorticity cut-offs over Europe, Q. J. R. Meteorol. Soc., 144, 701–719, https://doi.org/10.1002/qj.3239, 2018.

Puskeiler, M., Kunz, M., and Schmidberger, M.: Hail statistics for Germany derived from single-polarization radar data, Atmos. Res., 178–179, 459–470, https://doi.org/10.1016/j.atmosres.2016.04.014, 2016.

Quinting, J. F. and Vitart, F.: Representation of synoptic-scale Rossby wave packets and blocking in the S2S Prediction Project Database, Geophys. Res. Lett., 46, 1070–1078, https://doi.org/10.1029/2018GL081381, 2019.

Rädler, A. T., Groenemeijer, P., Faust, E., and Sausen, R.: Detecting severe weather trends using an Additive Regressive Convective Hazard Model (AR-CHaMo), J. Appl. Meteorl. Climatol., 57, 569–587, https://doi.org/10.1175/JAMC-D-17-0132.1, 2018.

Rasmussen, P. F. and Gautam, N.: Alternative PWM-estimators of the Gumbel distribution, J. Hydrol., 280, 265–271, https://doi.org/10.1016/S0022-1694(03)00241-5, 2003.

Rauthe, M., Steiner, H., Riediger, U., A., M., and Gratzki, A.: A Central European precipitation climatology – Part I: Generation and validation of a high-resolution gridded daily data set (HYRAS), Meteorol. Z., 22, 235–256, https://doi.org/10.1127/0941-2948/2013/0436, 2013.

Rex, D. F.: Blocking action in the middle troposphere and its effect upon regional climate: I. An aerological study of blocking action, Tellus, 2, 196–211, https://doi.org/10.3402/tellusa.v2i3.8546, 1950a.

Rex, D. F.: Blocking action in the middle troposphere and its effect upon regional climate: II. The climatology of blocking action, Tellus, 2, 275–301, https://doi.org/10.3402/tellusa.v2i4.8603, 1950b.

Roberts, N. M.: The relationship between water vapour imagery and thunderstorms, Joint Centre for Mesoscale Meteorology Internal Report No. 110, Met Office, Reading, UK, 2000.

Röthlisberger, M. and Martius, O.: Quantifying the local effect of Northern Hemisphere atmospheric blocks on the persistence of summer hot and dry spells, Geophys. Res. Lett., 43, 10 101–10 111, https://doi.org/10.1029/2019GL083745, 2019.

Röthlisberger, M., Martius, O., and Wernli, H.: Northern Hemisphere Rossby wave initiation events on the extratropical jet – A climatological analysis, J. Climate, 31, 743–760, https://doi.org/10.1175/JCLI-D-17-0346.1, 2018.

Russell, A., Vaughan, G., and Norton, E. G.: Large-scale potential vorticity anomalies and deep convection, Q. J. R. Meteorol. Soc., 138, 1627–1639, https://doi.org/10.1002/qj.1875, 2012.

Sánchez, J. L., Marcos, J. L., Dessens, J., López, L., Bustos, C., and García-Ortega, E.: Assessing sounding-derived parameters as storm predictors in different latitudes, Atmos. Res., 93, 446–456, https://doi.org/10.1016/j.atmosres.2008.11.006, 2009.

Santos, J. A. and Belo-Pereira, M.: A comprehensive analysis of hail events in Portugal: Climatology and consistency with atmospheric circulation, Int. J. Climatol., 39, 188–205, https://doi.org/10.1002/joc.5794, 2019.

Schaller, N., Sillmann, J., Anstey, J., Fischer, E. M., Grams, C. M., and Russo, S.: Influence of blocking on Northern European and Western Russian heatwaves in large climate model ensembles, Environ. Res. Lett., 13, 054 015, https://doi.org/10.1088/1748-9326/aaba55, 2018.

Schmidberger, M.: Hagelgefährdung und Hagelrisiko in Deutschland basierend auf einer Kombination von Radardaten und Versicherungsdaten, Ph.D. thesis, Wiss. Berichte d. Instituts für Meteorologie und Klimaforschung des Karlsruher Instituts für Technologie, Vol. 78, KIT Scientific Publishing, Karlsruhe, Germany, https://doi.org/10.5445/KSP/1000086012, 2018.

Schulz, W., Diendorfer, G., Pedeboy, S., and Poelman, D. R.: The European lightning location system EUCLID – Part 1: Performance analysis and validation, Nat. Hazards Earth Syst. Sci., 16, 595–605, https://doi.org/10.5194/nhess-16-595-2016, 2016.

Sivapalan, M. and Blöschl, G.: Transformation of point rainfall to areal rainfall: Intensity-duration-frequency curves, J. Hydrol., 204, 150–167, https://doi.org/10.1016/S0022-1694(03)00241-5, 1998.

Sousa, P. M., Trigo, R. M., Barriopedro, D., Soares, P. M. M., Ramos, A. M., and Liberato, M. L. R.: Responses of European precipitation distributions and regimes to different blocking locations, Clim. Dynam., 48, 1141–1160, https://doi.org/10.1007/s00382-016-3132-5, 2017.

Sprenger, M. and Wernli, H.: The LAGRANTO Lagrangian analysis tool–version 2.0, Geosci. Model Dev., 8, 2569–2586, https://doi.org/10.5194/gmd-8-2569-2015, 2015.

Sprenger, M., Fragkoulidis, G., Binder, H., Croci-Maspoli, M., Graf, P., Grams, C. M., Knippertz, P., Madonna, E., Schemm, S., Škerlak, B., and Wernli, H.: Global climatologies of Eulerian and Lagrangian flow features based on ERA-Interim, Bull. Am. Meteorol. Soc., 98, 1739–1748, https://doi.org/10.1175/BAMS-D-15-00299.1, 2017.

Tarabukina, L. D., Antokhina, O. Y., Kononova, N. K., Kozlov, V. I., and Innokentiev, D. E.: Formation of intense thunderstorms in Yakutia in periods of frequent atmospheric blocking in Western Siberia, in: IOP Conf. Ser.: Mater. Sci. Eng., vol. 698, p. 044050, https://doi.org/10.1088/1757-899x/698/4/044050, 2019.

Thompson, R. L., Mead, C. M., and Edwards, R.: Effective storm-relative helicity and bulk shear in supercell thunderstorm environments, Weather Forecast., 22, 102–115, https://doi.org/10.1175/WAF969.1, 2007.

Tibaldi, S. and Molteni, F.: On the operational predictability of blocking, Tellus A, 42, 343–365, https://doi.org/10.1034/j.1600-0870.1990.t01-2-00003.x, 1990.

Trapp, R. J.: Mesoscale-convective processes in the atmosphere, Cambridge University Press, New York, USA, 2013.

van Delden, A.: The synoptic setting of thunderstorms in Western Europe, Atmos. Res., 56, 89–110, https://doi.org/10.1016/S0169-8095(00)00092-2, 2001.

van den Besselaar, E. J. M., Klein Tank, A. M. G., and Buishand, T. A.: Trends in European precipitation extremes over 1951–2010, Int. J. Climatol., 33, 2682–2689, https://doi.org/10.1002/joc.3619, 2013.

Vautard, R.: Multiple weather regimes over the North Atlantic: Analysis of precursors and successors, Mon. Weather Rev., 118, 2056–2081, https://doi.org/10.1175/1520-0493(1990)118<2056:MWROTN>2.0.CO;2, 1990.

Wapler, K.: High-resolution climatology of lightning characteristics within Central Europe, Meteorol. Atmos. Phys., 122, 175–184, https://doi.org/10.1007/s00703-013-0285-1, 2013.

Wapler, K. and James, P.: Thunderstorm occurrence and characteristics in Central Europe under different synoptic conditions, Atmos. Res., 158, 231–244, https://doi.org/10.1016/j.atmosres.2014.07.011, 2015.

Weisman, M. L. and Klemp, J. B.: The dependence of numerically simulated convective storms on vertical wind shear and buoyancy, Mon. Weather Rev., 110, 504–520, https://doi.org/10.1175/1520-0493(1982)110<0504:TDONSC>2.0.CO;2, 1982.

Wernli, H. and Davies, H. C.: A Lagrangian-based analysis of extratropical cyclones. I: The method and some applications, Q. J. R. Meteorol. Soc., 123, 467–489, https://doi.org/10.1002/qj.49712353811, 1997.

Wernli, H. and Sprenger, M.: Identification and ERA-15 climatology of potential vorticity streamers and cutoffs near the extratropical tropopause, J. Atmos. Sci., 64, 1569–1586, https://doi.org/10.1175/JAS3912.1, 2007.

Westermayer, A. T., Groenemeijer, P., Pistotnik, G., Sausen, R., and Faust, E.: Identification of favorable environments for thunderstorms in reanalysis data, Meteorol. Z., 26, 59–70, https://doi.org/10.1127/metz/2016/0754, 2017.

WetterOnline: Tornado wütet bei Viersen: Dutzende Häuser stark beschädigt (17.05.2018), WetterOnline Meteorologische Dienstleistungen GmbH, Bonn, Germany. Available from: https://www.wetteronline.de/extremwetter/tornado-wuetet-bei-viersen-dutzende-haeuser-stark-beschaedigt-2018-05-17-tv (Accessed 13 March 2020), 2018a.

WetterOnline: Unwetterserie Ende Mai: Ganze Ortschaften verwüstet, WetterOnline Meteorologische Dienstleistungen GmbH, Bonn, Germany. Available from: https://www.wetteronline.de/extremwetter/unwetterserie-ende-mai-ganze-ortschaften-verwuestet-2018-05-31-us (Accessed 13 March 2020), 2018b.

WetterOnline: Unwetterserie im Juni: Überflutungen und Hagelmassen (14.06.2018), WetterOnline Meteorologische Dienstleistungen GmbH, Bonn, Germany. Available from: https://www.wetteronline.de/extremwetter/unwetterserie-im-juni-ueberflutungen-und-hagelmassen-2018-06-14-js (Accessed 13 March 2020), 2018c.

Wilks, D. S.: Statistical methods in the atmospheric sciences: An introduction – Second Edition, Academie Press, Elsevier, Burlington, USA, 2006.

Wilson, J. W. and Schreiber, W. E.: Initiation of convective storms at radar-observed boundary-layer convergence lines, Mon. Weather Rev., 114, 2516–2536, https://doi.org/10.1175/1520-0493(1986)114<2516:IOCSAR>2.0.CO;2, 1986.

Woollings, T., Barriopedro, D., Methven, J., Son, S.-W., Martius, O., Harvey, B., Sillmann, J., Lupo, A. R., and Seneviratne, S.: Blocking and its response to climate change, Curr. Clim. Change Rep., 4, 287–300, https://doi.org/10.1007/s40641-018-0108-z, 2018.

Wussow, G.: Untere Grenzwerte dichter Regenfälle, Meteorol. Z., 39, 173–178, 1922.

Table 1. **Top list of 1 h, 3 h, and 24 h rainfall totals (in UTC) within the study domain during the study period (AT = Austria, FR = France, GE = Germany). Note that 24 h value means precipitation between 00 and 00 UTC on the next day. Note that some stations only provide reports for the full 24 hours (e.g., Bruchweiler; Mauth-Finsterau). Further analyses regarding rain duration (RD), track length (in km), propagation speed (in m s^{-1}), and total track area (in km^2) are limited to Germany due to data availability. RD3 means a rain duration with a rain rate > 3 mm h^{-1}, RD35 > 35 mm h^{-1}, and RD60 > 60 mm h^{-1}. Note two tracks for the German events could not be identified by TRACE3D due to the overlapping of several cells, which were relatively quasi-stationary**.

Period	Location (Country)	Coordinates	Rainfall	Time	RD3	RD35	RD60	Length	Speed	Area
1 h	Dietenhofen (GE)	49.4°N 10.7°E	85.7 mm	31 May 19 h	1 h	45 min	35 min			
1 h	Rohr-Dechendorf (GE)	49.3°N 10.9°E	71.0 mm	09 June 15 h	1 h	40 min	15 min	84	15	608
1 h	Labécède-Lauragais (FR)	43.4°N 2.0°E	64.4 mm	10 June 17 h						
1 h	Hohenberg an der Eger (GE)	50.1°N 12.2°E	61.4 mm	31 May 18 h	1 h	55 min	30 min	30	6.6	215
1 h	Lenzkirch-Ruhbühl (GE)	47.9°N 8.2°E	59.8 mm	31 May 20 h	40 min	30 min	20 min			
1 h	Langres (FR)	47.8°N 5.3°E	59.4 mm	05 June 20 h						
1 h	Castanet-le-Haut (FR)	43.7°N 3.0°E	56.2 mm	30 May 14 h						
1 h	Erlbach-Eubabrunn (GE)	50.3°N 12.4°E	55.6 mm	31 May 17 h	1 h	50 min	35 min	25	4.4	190
1 h	Rouvroy-en-Santerre (FR)	49.8°N 2.7°E	54.3 mm	28 May 22 h						
3 h	Prades-le-Lez (FR)	43.7°N 3.9°E	86.8 mm	11 June 15 h						
3 h	Bad Elster-Sohl (GE)	50.3°N 12.3°E	86.3 mm	24 May 15 h	3 h	25 min	0 min	16.5	4.6	105
3 h	Puchberg am Schneeberg (AT)	47.8°N 15.9°E	86.3 mm	12 June 15 h						
3 h	Dietenhofen (GE)	49.4°N 10.7°E	86.2 mm	31 May 21 h	∼ 1 h 25 min	45 min	35 min			
3 h	L'Oudon-Lieury (FR)	49.0°N 0.0°E	83.8 mm	28 May 15 h						
3 h	Rocroi (FR)	49.9°N 4.5°E	79.4 mm	27 May 21 h						
3 h	Leutkirch-Herlazhofen (GE)	47.8°N 10.0°E	79.1 mm	08 June 18 h	∼ 2 h 30 min	45 min	20 min	8.7	3.2	42
3 h	Kleve (GE)	51.8°N 6.1°E	78.8 mm	29 May 18 h	∼ 2 h 45 min	40 min	20 min	14.5	5.4	70
3 h	Sulzberg (AT)	47.5°N 9.9°E	78.0 mm	04 June 18 h						
24 h	Mauth-Finsterau (GE)	48.9°N 13.6°E	166.5 mm	12 June	∼ 8 h 0 min	55 min	20 min	9.2	3.4	44
24 h	Bad Elster-Sohl (GE)	50.3°N 12.3°E	154.9 mm	24 May	∼ 8 h 15 min	20 min	0 min	16.5	4.6	105
24 h	Bruchweiler (GE)	49.8°N 7.2°E	145.0 mm	27 May	∼ 2 h 30 min	1 h 5 min	50 min	20.5	5.7	130
24 h	Monein (FR)	43.3°N 0.5°W	130.0 mm	12 June						
24 h	Ger (FR)	43.2°N 0.1°W	126.4 mm	12 June						
24 h	Mont Aigoual (FR)	44.1°N 3.6°E	124.1 mm	28 May						
24 h	Les Bottereaux (FR)	48.9°N 0.7°E	123.0 mm	04 June						
24 h	Navarrenx (FR)	43.3°N 0.8°W	117.0 mm	12 June						
24 h	Puchberg am Schneeberg (AT)	47.8°N 15.9°E	116.3 mm	12 June						

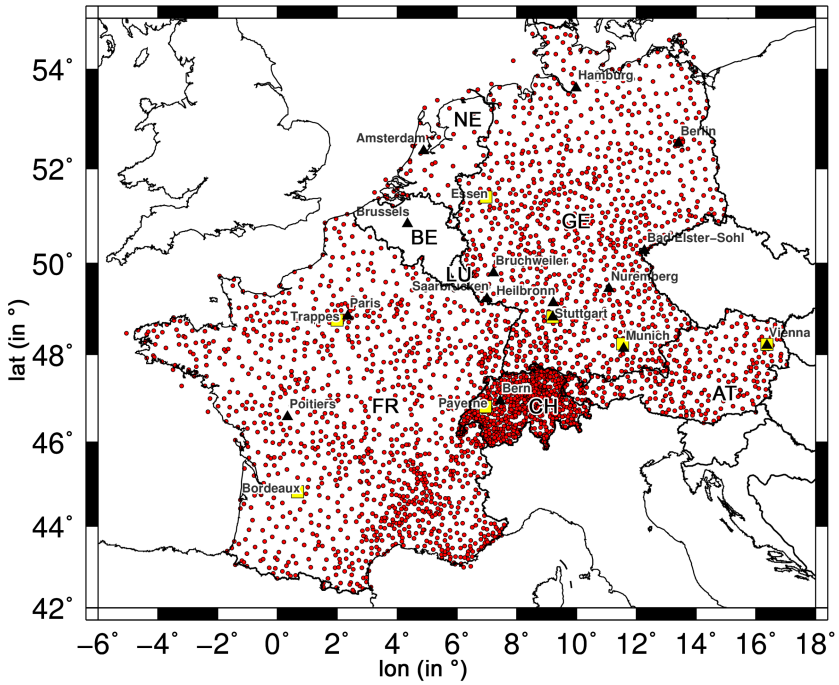

Figure 1. All considered precipitation stations (in red) collected from ECA&D and the three national weather services (France, Germany, Switzerland; see Sect. 2.1.3). In addition, the seven investigated sounding stations are shown (in yellow, see Sect. 2.1.5). Some relevant locations are also presented, which are used in the text. Defined country codes are FR = France, BE = Belgium, NE = Netherlands, LU = Luxembourg (the latter three: Benelux), GE = Germany, CH = Switzerland, AT = Austria.

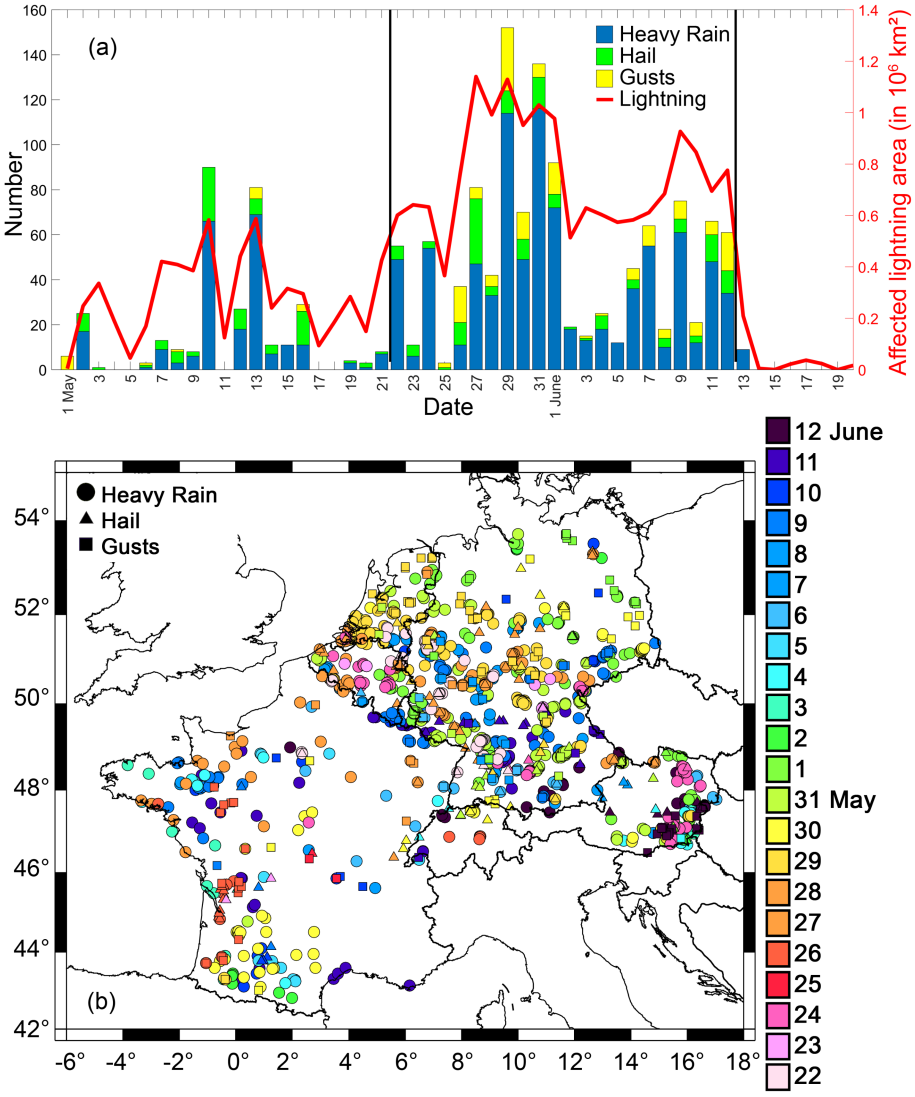

Figure 2. (a) Time series of all recorded ESWD reports (heavy rain in blue, hail in green, convective gusts in yellow) in the study domain during the extended study period including the daily total area affected by lightning in km^2 (in red). **Vertical black lines indicate the study period (22 May to 12 June 2018)**. (b) Related regional distribution of the different phenomena (heavy rain ●, hail ▲, convective gusts ■) during the study period.

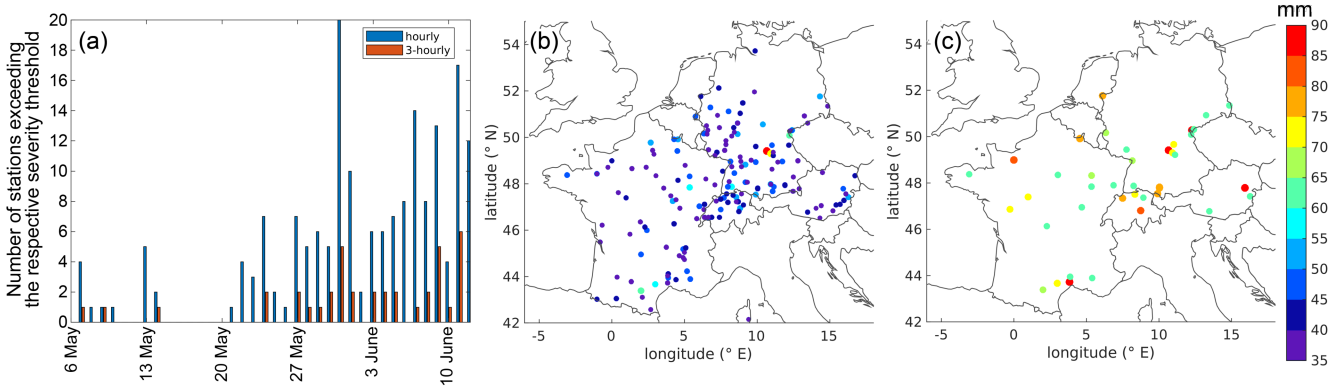

Figure 3. **(a) Time series of the number of stations exceeding precipitation thresholds of >35 mm hourly (blue) and >60 mm over 3-hours (red) including the location and total maximum of (b) hourly and (c) 3-hour sums of the respective station during the study period (22 May to 12 June).**

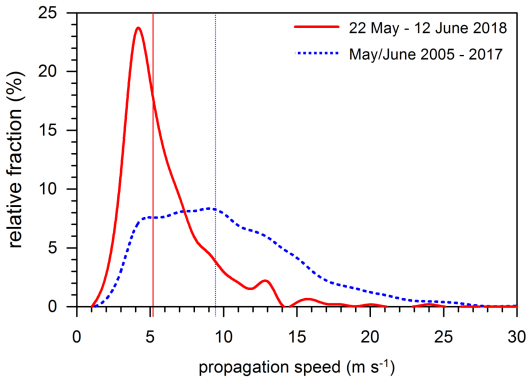

Figure 4. Histogram of the propagation speed of convective cells (increments of 1 m s^{-1}; spline filter) detected by TRACE3D in Germany during the study period (red) and for all convective cells between 2005 and 2017 (May/June; blue); vertical lines indicate the median of the two samples.

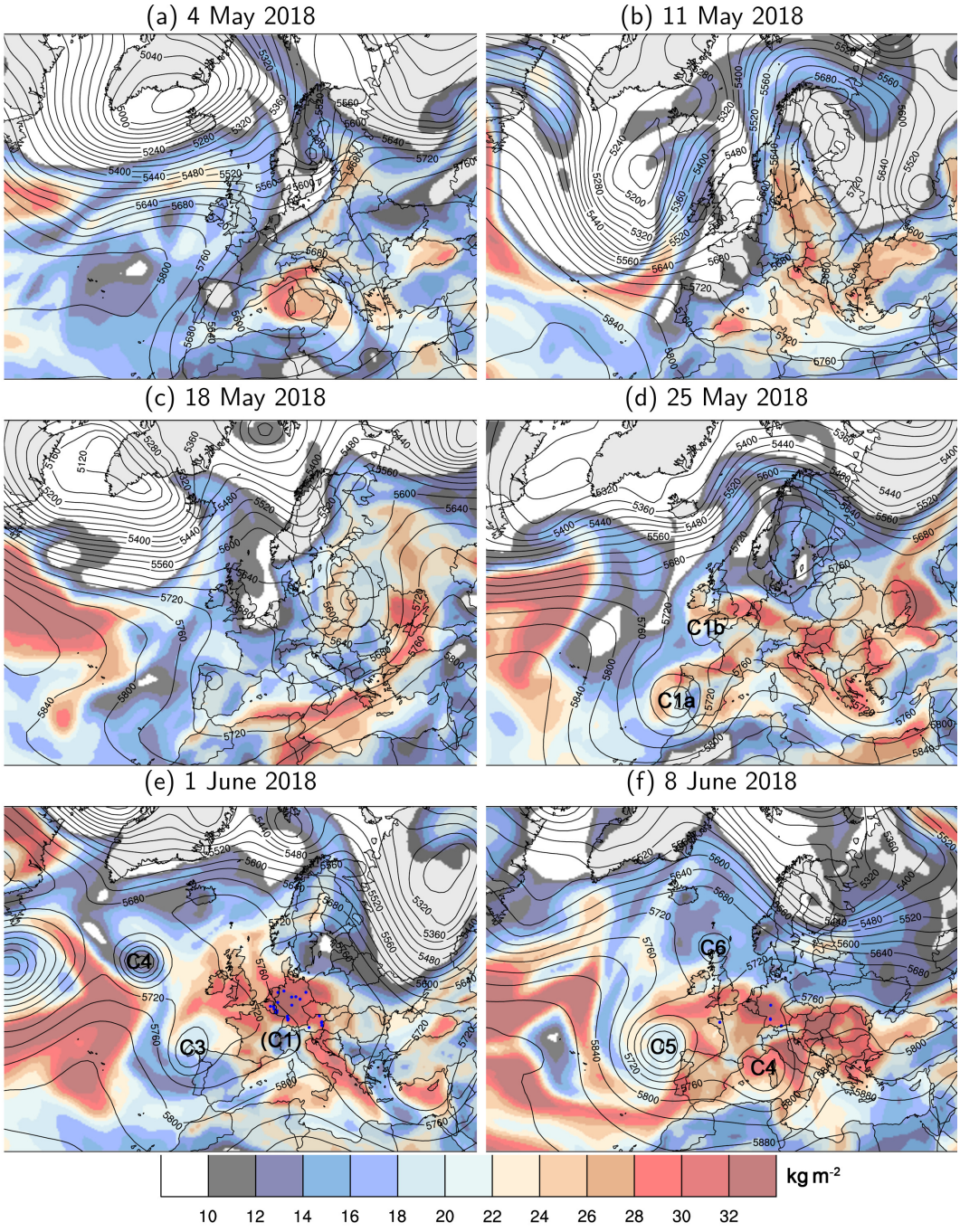

Figure 5. 500 hPa geopotential height (contours every 40 gpm) and vertically integrated water vapor (IWV, shaded in kg m^{-2}) for selected days at 00 UTC during the extended study period: (a) 4 May, (b) 11 May, (c) 18 May, (d) 25 May, (e) 1 June, and (f) 8 June (ERA-Interim). Several cut-off lows during the study period mentioned in the text are indicated with numbers (C1, ..., C6). **Small blue dots (in e and f) mark the ESWD reports on heavy rain from Fig. 2. Note that there are no ESWD reports for the first four panels.**

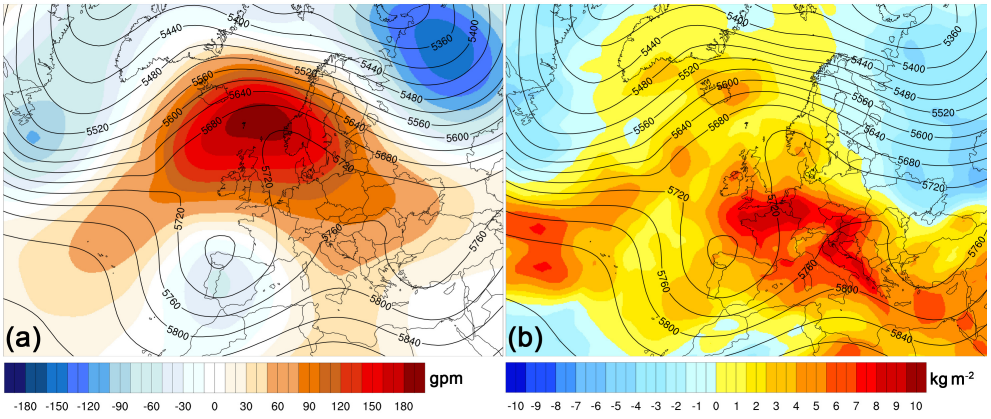

Figure 6. Composite mean 500 hPa geopotential height (contours every 40 gpm) and in (a) anomaly with reference the climatological mean in May and June (1981 – 2010; shaded in gpm) and in (b) together with anomalies of the IWV with reference to the climatological mean in May and June (1981 – 2001; shaded in kg m^{-2} (based on ERA-Interim).

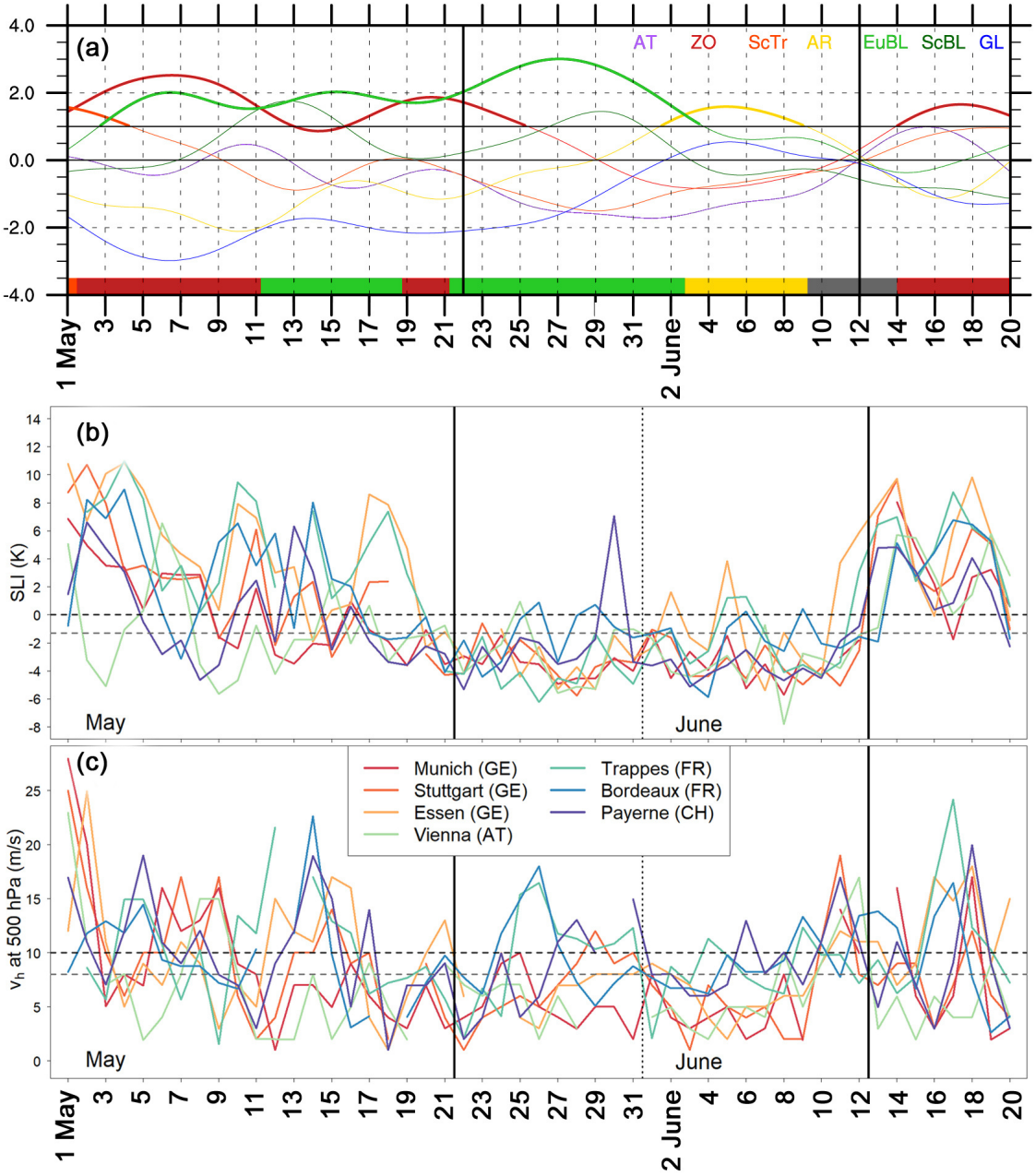

Figure 7. **Time series of three different parameters during the extended study period from 1 May to 20 June 2018: (a) Atlantic-European weather regime life cycles including normalized projection into all seven regimes (ECMWF analysis). Active regimes (according to the life cycle definition in bold) are Zonal regime (ZO, dark red), European Blocking (EuBL, light green), Atlantic Ridge (AR, yellow), no regime (grey; see text for details). (b) Surface-based Lifted Index (SLI in K) and (c) horizontal wind speed at 500 hPa (V500 in m s^{-1}) for the 12 UTC sounding at seven European stations. Horizontal black/gray dashed lines indicate thresholds as defined in PIP16 (Basic criterion: 0 K & 10 m s^{-1}; Strict criterion: -1.3 K & 8 m s^{-1}; cf. Sect. 2.6). Vertical black lines indicate the study period.**

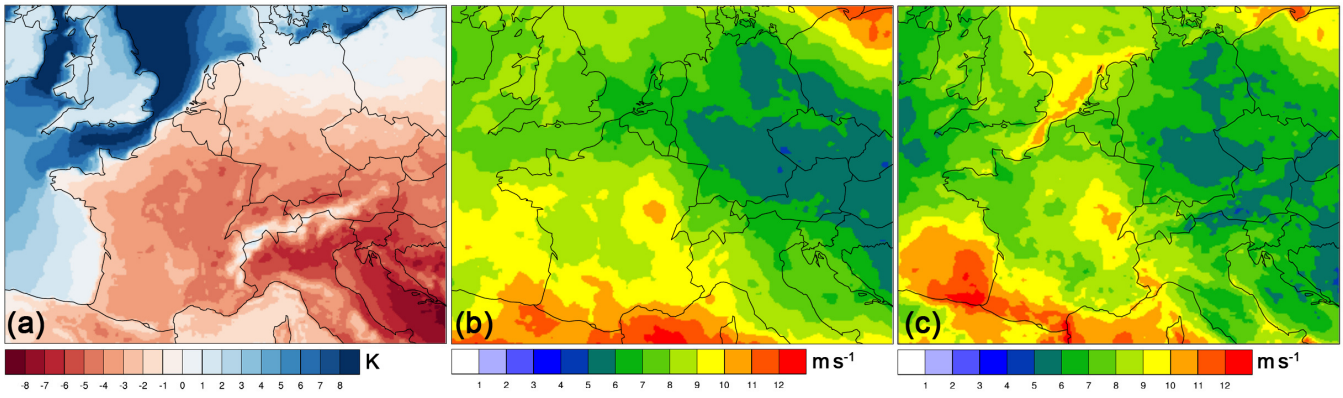

Figure 8. (a) Surface-based Lifted Index (SLI in K), (b) horizontal wind speed at 500 hPa (V500 in $\mathrm{m\,s^{-1}}$), and (c) bulk wind shear between 500 hPa and 10 m (BWS in $\mathrm{m\,s^{-1}}$) averaged over the study period from 22 May to 12 June 2018 (12 UTC; ECMWF analysis).

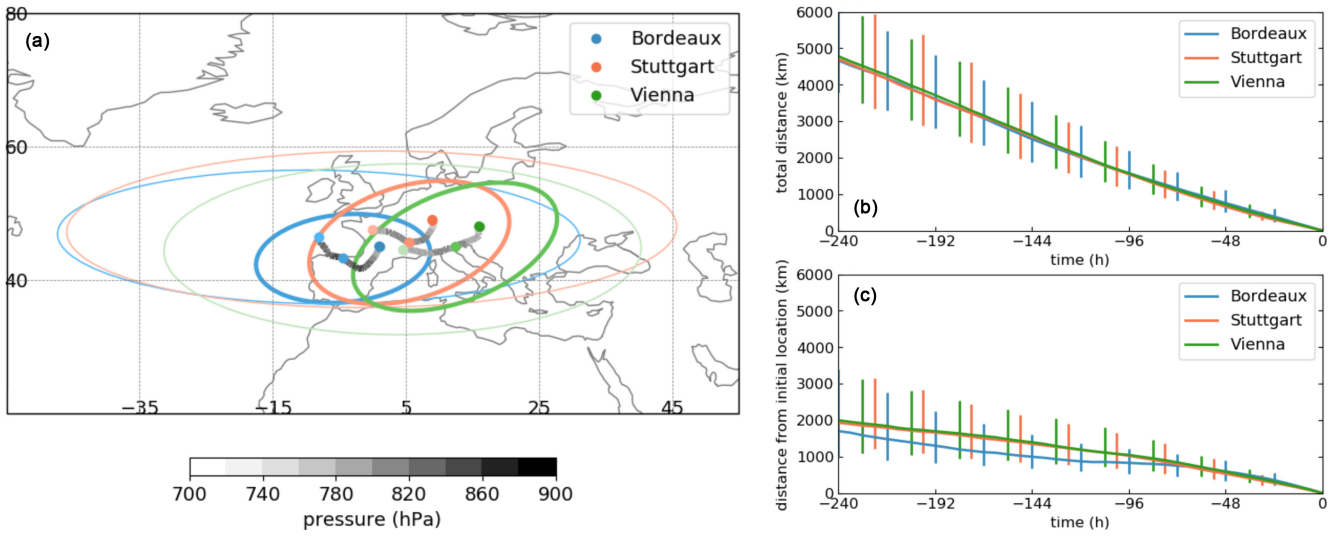

Figure 9. 10-day backward trajectory analysis from 22 May to 12 June 2018. (a) Median backward trajectories coloured by their median pressure (hPa) for three locations given in legend. The ellipses show the dispersion of the trajectories around their median location (dots) at 10 days (thin ellipses) and 5 days (bold ellipses) prior to arriving at the location. The ellipses enclose about 2/3 of the trajectories. (b) Temporal evolution of median distance travelled by the trajectories (km) prior to arriving at one of the locations given in legend. Bars show the interquartile range. (c) As in (b), but for distance from the initial location.

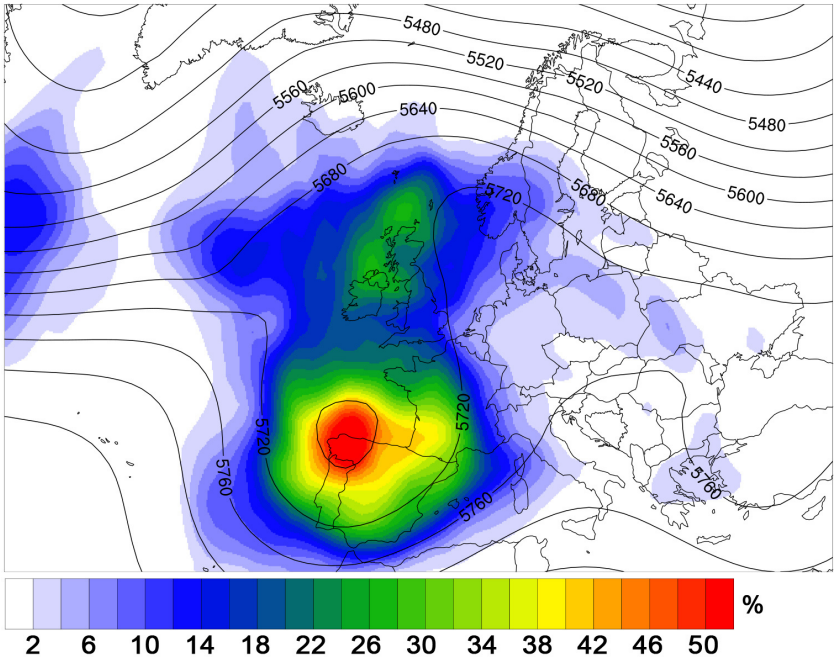

Figure 10. Composite mean of 500 hPa geopotential height (contours every 40 gpm) and cut-off low frequency (color shading in %) during the study period (ERA-Interim).

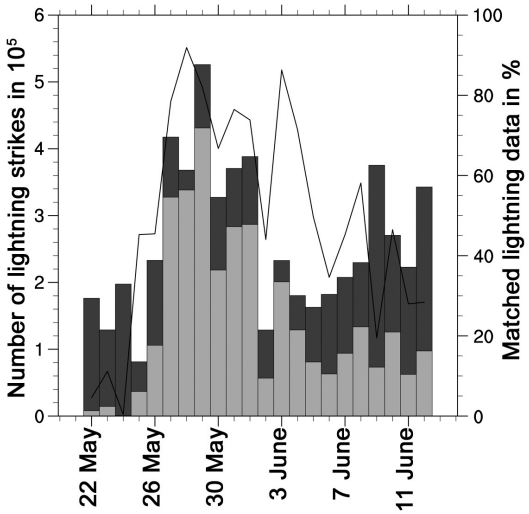

Figure 11. Lightning strikes per day (03 UTC – 03 UTC on the next day) during the study period for all thunderstorm events (dark grey bars) and those thunderstorms that can be linked to a cut-off low (light grey bars). The black line shows the percentage of lightning strikes per day that can be attributed to a cut-off low.

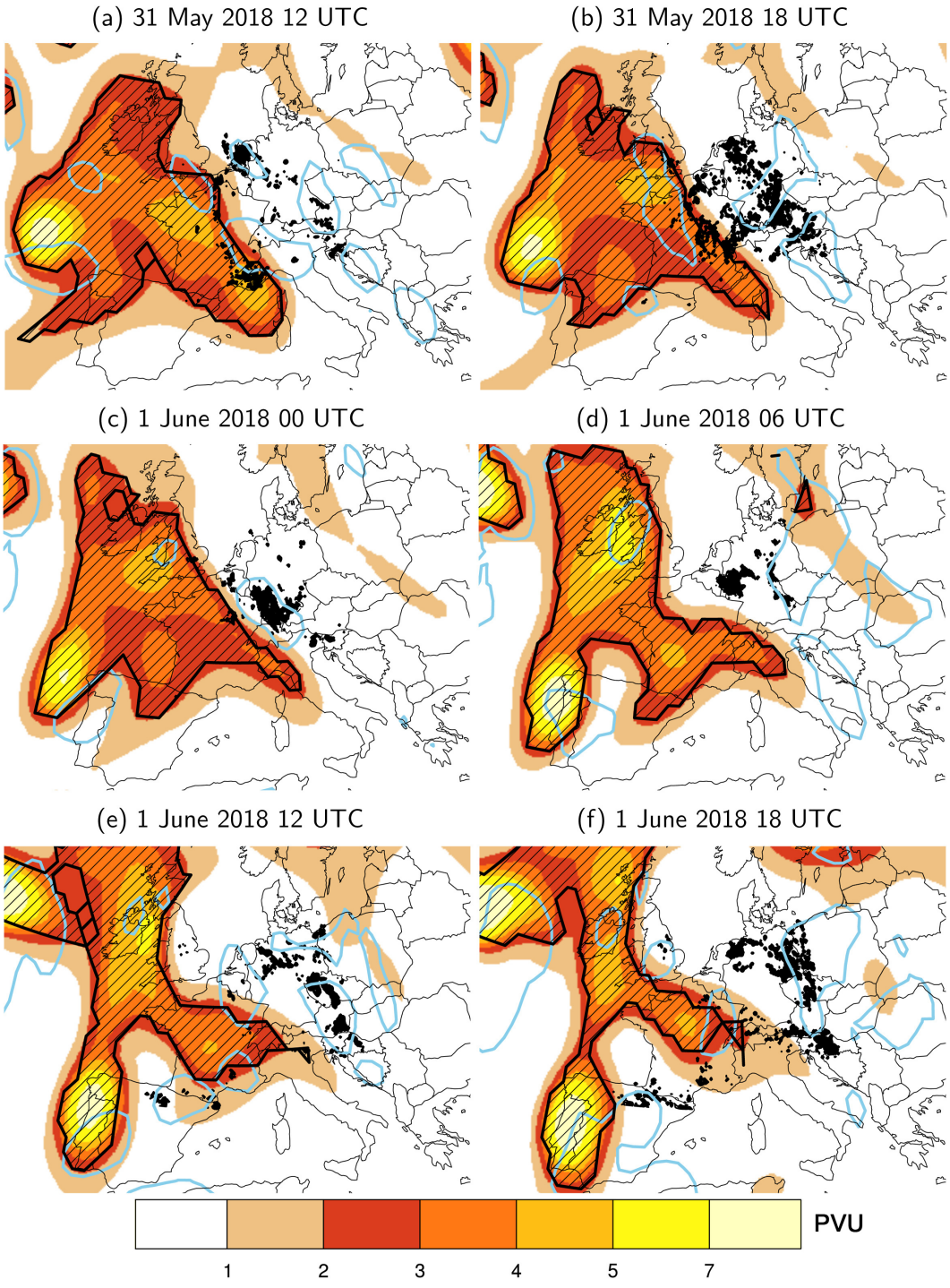

Figure 12. Lightning data (dark black dots) for 6-hour time spans centered around the respective time and PV on the 325 K isentropic surface (shaded in PVU; ERA-Interim). Regions of ascent at 500hPa are indicated by **light blue** contours ($\omega = -0.1$ Pa s^{-1}); ERA-Interim). Hatching indicates masks of objectively identified cut-offs on the 325 K isentropic surface **(See Supplementary Fig. 2 including the buffer zone.)**

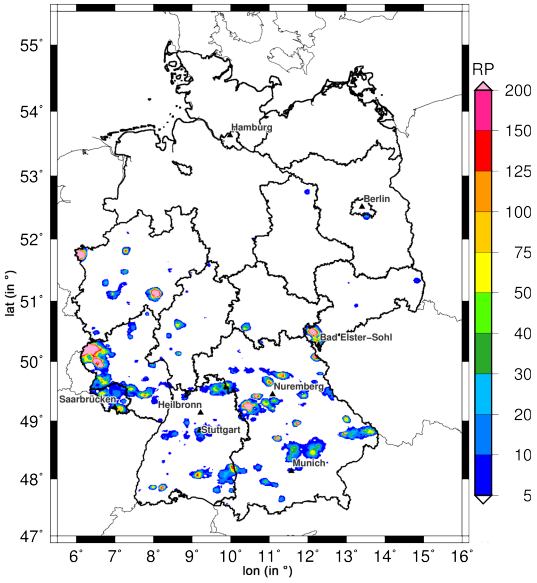

Figure 13. Return periods (RP) of the highest 24-hour **rainfall totals** that occurred during the study period at each grid point (REGNIE precipitation data; reference period: 1951 – 2017, summer half-year).

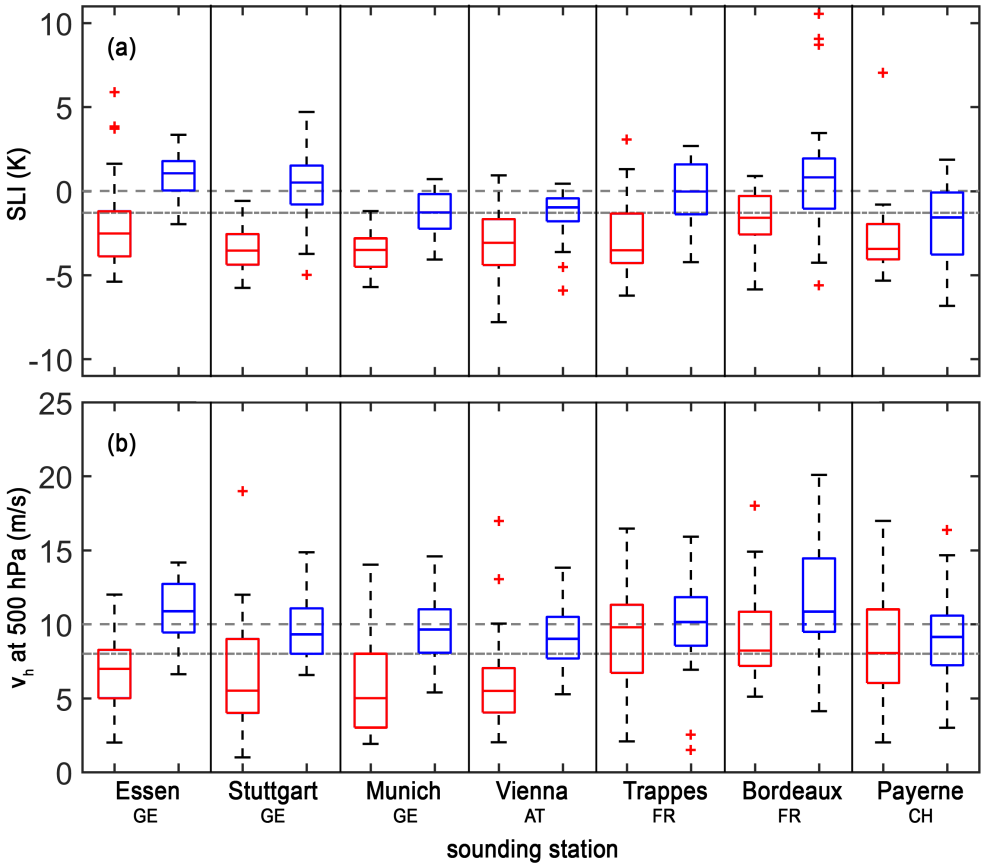

Figure 14. Box-and-whisker plots (median, 1st/3rd quartiles, whisker = +/–2.7σ, outliers) for the seven sounding stations. The left box-plots **(in red)** of each station include all values of (a) SLI and (b) V500 during the study period at 12 UTC, the right box-plots **(in blue)** include the annual minimum of the running mean (22 days) during May and June between 1981 and 2010. The two gray lines **indicate thresholds as defined in PIP16 (Basic criterion: 0 K & 10 m s^{-1}; Strict criterion: -1.3 K & 8 m s^{-1}; cf. Sect. 2.6). Note that the median on the left box-and-whisker plots is calculated identically as all 30 values in the right box-and-whisker plots.**

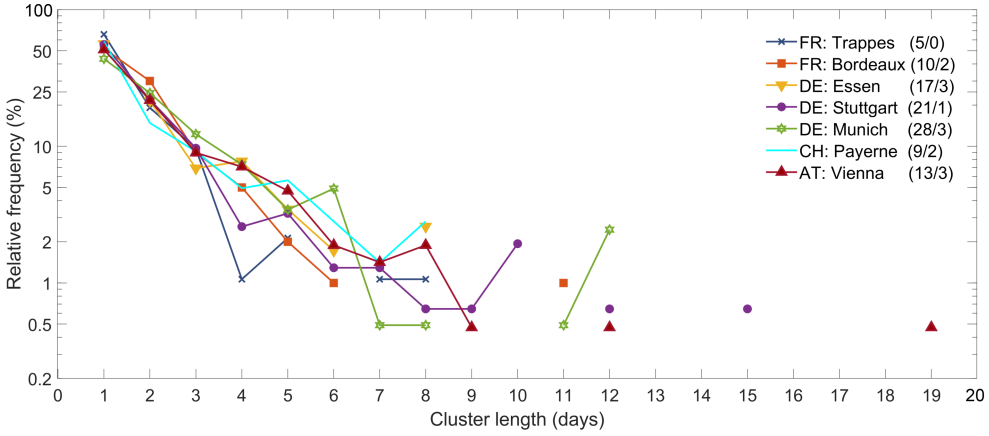

Figure 15. Relative frequency of clusters of consecutive days exceeding the basic criterion for concurrent events with low stability (SLI < 0 K) and weak flow (V500 < 10 m s^{-1}) at the seven sounding stations (Trappes, Bordeaux, Essen, Stuttgart, Munich, Payerne, Vienna) during 1981 – 2017 (May/June). Maximum days with **event persistence n (including skip days m) during the extended study period in 2018 (Mai/June) are shown in the legend (n/m)**.

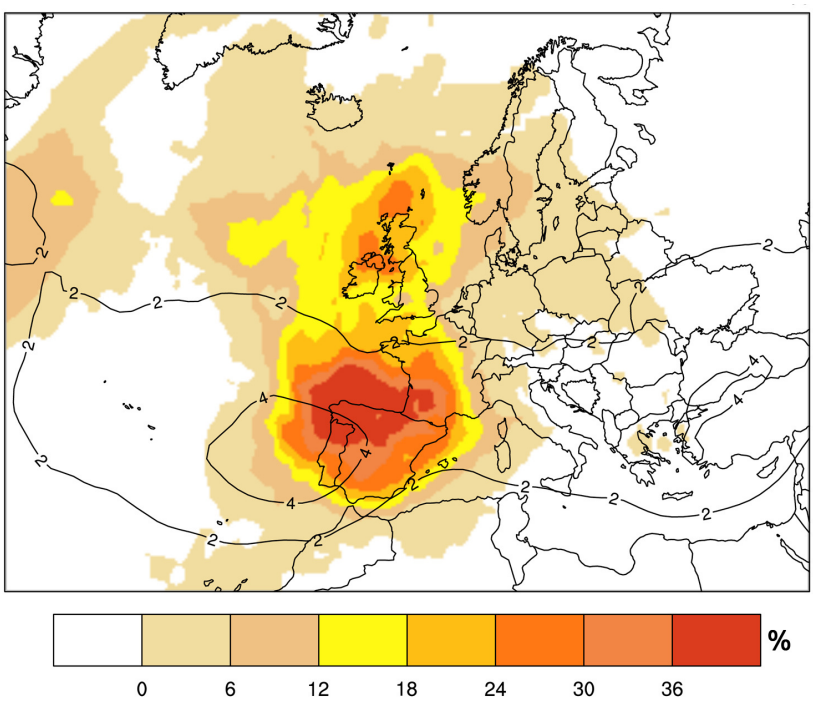

Figure 16. **Climatological mean percentage of days with a cut-off low in May and June (black contours; every 2 %; for May and June 1981 – 2010) and anomaly percentage of days during the study period (shaded in % with reference to mean percentage of days** in May and June; ERA-Interim).